National Défense
Defence nationale

EVALUATION OF THE FMICW WAVEFORM IN HF SURFACE WAVE RADAR APPLICATIONS

by

H.C. Chan

DEFENCE RESEARCH ESTABLISHMENT OTTAWA
REPORT N0. 1219

Canada

January 1994
Ottawa

National Défense
Defence nationale

EVALUATION OF THE FMICW WAVEFORM IN HF SURFACE WAVE RADAR APPLICATIONS

by

H.C. Chan
Surface Radar Section
Radar and Space Division

DEFENCE RESEARCH ESTABLISHMENT OTTAWA
REPORT N0. 1219

PCN
041LR

January 1994
Ottawa

ABSTRACT

The operation and performance of the Frequency Modulated Interrupted Continuous Wave (FMICW) waveform in ship and aircraft detection using high frequency surface wave radar are analyzed. A modified processing scheme for the FMICW waveform which circumvents the problem of ambiguous range response is presented. The increase in hardware complexity for the modified processing scheme is moderate.

Two measures: (a) the signal-to-clutter ratio and (b) the signal-to-noise ratio are used to evaluate the performance of the FMICW. It is concluded that the FMICW is superior to the simple pulsed waveform in ship-detection application.

For aircraft detection, the advantage of the FMICW is marginal. Parameters optimized for ship-detection application will not be optimal for aircraft-detection application because of their much higher velocity which exacerbates the range-walk problem.

RÉSUMÉ

Nous analysons le fonctionnement et la performance de l'onde entretenue interrompue à modulation de fréquence pour la détection de bateaux et d'avions par un radar transhorizon à ondes décamétriques. Nous présentons une version modifiée de la méthode de traitement de l'onde entretenue interrompue à modulation de fréquence qui élimine le problème d'ambiguïté en distance. L'augmentation de complexité en matériel est modérée avec cette modification.

La performance de l'onde entretenue interrompue à modulation de fréquence est évaluée selon deux critères: (a) le rapport signal-sur-fouillis et (b) le rapport signal-sur-bruit. Nous concluons que l'utilisation de l'onde entretenue interrompue à modulation de fréquence donne des résultats supérieurs à celle d'une simple onde pulsée lors de la détection des bateaux.

L'avantage de l'onde entretenue interrompue à modulation de fréquence est marginal pour la détection d'avions. Les paramètres, optimisés pour la détection de bateaux, ne sont pas optimaux pour la détection d'avions à cause de leur vitesse beaucoup plus grande ce qui amplifie le problème de migration des cibles vers les cellules de portée voisines.

EXECUTIVE SUMMARY

High frequency surface wave radar (HFSWR) offers an economical means of monitoring wide areas of the ocean for surface–vessel and aircraft traffic. There are, however, some limitations to the utilization of these radars. To overcome these limitations, optimal designs in antenna, transmit waveform, receiver and signal processors are required. In this report we examine the utilization of the Frequency Modulated Interrupted Continuous Wave (FMICW) waveform for HFSWR for the purpose of detecting ships and aircraft. Particular attention has been paid to the performace of the waveform in the presence of sea clutter and external noise. Conventional approach to processing FMICW signal produces ambiguous range response and related problems. A modified processing scheme for the FMICW waveform which circumvents these problems is presented. The increase in hardware complexity for the modified processing scheme is moderate.

The performance of the FMICW waveform in ship and aircraft detection applications is evaluated against a conventional pulse Doppler waveform. Two performance measures are used: (a) the signal–to–clutter ratio and (b) the signal–to–noise ratio. It is concluded that the FMICW is superior to the simple pulsed waveform in ship–detection application because it enhances the signal–to–clutter ratio, provides a finer range resolution and requires a lower peak power.

For aircraft detection, the advantage of the FMICW is perhaps marginal. It depends on the parameters chosen for the system. Generally the FM sweep rate and the sweep period must be chosen so that the resulting Doppler bandwidth would be unambiguous for the anticipated aircraft speed. Parameters optimized for ship–detection application will not be optimal for aircraft–detection application because of their much higher velocity which exacerbates the range–walk problem. Attempts to circumvent the range–walk problem by signal processing means will increase the complexity and processing time to the extent that it negates the possible performance improvement of the FMICW waveform over that of the simple pulse Doppler waveform.

Table of Contents

Table of Contents (Continue)

LIST OF FIGURES

1. Introduction

There is a considerable amount of interest, both in the defence and remote sensing communities, in employing High Frequency Surface Wave Radar (HFSWR) for long range coastal surveillance applications. HFSWR offers an economical means of monitoring wide areas of the ocean for surface–vessel and aircraft traffic. There are, however, some limitations to the utilization of these radars. First, the wavelength at the High Frequency (HF) region (2 MHz to 30 MHz) ranges from 10 m to 150 m. To produce an antenna beam of moderate beamwidth (a few degrees), a large antenna aperture is required. This means that HF radars usually have poor angular resolution. Second, the extent of the entire HF band is in the order of 30 MHz and is very congested. This severely limits the bandwidth of the signal that can be employed. As a result, the range–resolution capability of HFSWR is generally limited. Typically HFSWR signal bandwidths are in the order of several tens of kHz. Third, signals propagate in the surface wave mode are subjected to an additional propagation loss [1] that increases with range and with frequency. Consequently, reliable detection of targets requires a tremendous amount of signal processing gain. An effective HFSWR requires optimal designs in antenna, transmit waveform, receiver and signal processing. In this report we examine the utilization of the Frequency Modulated Interrupted Continuous Wave (FMICW) waveform for HFSWR for the purpose of detecting ships and aircraft. Particular attention will be paid to the evaluation of the performance of the waveform in the presence of sea clutter and external noise. Where possible the performance will be compared with that of an unmodulated pulse waveform. Section 2 provides some background on the waveforms being considered and the signal processing required to extract target information. A modified processing scheme for the FMICW waveform which circumvents some of the problems encountered in the standard processing method is presented. Section 3 examines the effects of the waveform on sea clutter and noise. Section 4 summaries the findings and presents the appropriate conclusions.

2. Pulsed FM, FMCW and FMICW waveforms.

The simple unmodulated pulse, the frequency modulated continuous wave (FMCW) and the FMICW are three of the commonly used waveforms in HF radars. The operation of the unmodulated pulse waveform is straightforward, and its performance is relatively well understood. The operation and performance characteristics of the two FM waveforms are more complicated and dependent upon the target and interference characteristics.

In this report we are interested primarily in the performance of the FMICW. Before introducing the FMICW, it would be useful to review some background information on FM signals, and in particular, the related FMCW signal. We shall restrict the discussion to the special class of linear FM signals. The optimal processing of FM radar signals is well documented [2–6], therefore we shall not present the detailed theory. Nevertheless, some of the pertinent results and concepts such as range–Doppler ambiguity, time–bandwidth product and pulse–compression–ratio will be presented. These are used to facilitate the evaluation of the merits of employing the FMICW in HFSWR relative to those of a simple pulsed waveform.

In radar and communications work, one usually deals with narrow–band signals in the sense that the signal spectrum is concentrated in the vicinity of the carrier frequency. A modulated signal at radio frequency (RF) is represented mathematically as:

$$s(t) = A(t)\cos[2\pi f_o t + \phi(t)] \tag{1}$$

where f_o, $A(t)$ and $\phi(t)$ are the carrier frequency, amplitude and phase of the signal, respectively. Equation (1) may be rewritten in complex exponential form as:

$$s(t) = Re\{A(t)\exp[j\phi(t)]\exp(j2\pi f_o t)\} \tag{2}$$

where $Re\{\ \}$ signifies the real part of a complex quantity.

For narrow band signals, the variation of the amplitude $A(t)$ from one cycle of the carrier to the next is small. Under this condition, it is valid to consider the equivalent complex baseband function of a band–pass signal:

$$u(t) = A(t)\exp[j\phi(t)]. \tag{3}$$

Signal processing operations such as band–pass filtering to be performed on a narrow–band signal can be performed using equivalent complex baseband operations because virtually all the information is contained in u(t); the presence of the carrier $\exp(j2\pi f_o t)$ merely translates the signal spectrum along the frequency axis. In subsequent discussions, we shall use the complex exponential representation to describe narrow–band modulated signals.

2.1 Pulsed Linear Frequency Modulation (FM) Waveform.

The pulsed linear FM signal is commonly used in microwave pulse compression radars to provide improved range resolution with substantially lower peak power requirement than an equivalent pulsed waveform without modulation. A linear FM pulse is a sinusoidal signal of moderate duration within which the carrier frequency varies linearly with time. The complex baseband representation of a linear FM pulse [2] is:

$$u(t) = A \exp(j\pi\mu t^2) \qquad (4)$$

$$0 \leq t \leq T$$

where amplitude A is constant, μ is the frequency sweep rate in Hz/sec, and T is the length of the pulse in seconds. Since the frequency is swept at a rate of μ Hz/sec, in T seconds the change in the carrier frequency is:

$$B = \mu T \qquad (5)$$

We call B the sweep bandwidth of the linear FM signal.

Assume that there is a point target located at a distance R from the radar. When a pulse is transmitted, an echo will be returned from the point target. The time required for the echo to arrive at the radar is given by τ:

$$\tau = \frac{2R}{c} \tag{6}$$

where c is the speed of light.

Eclipsing distance

If τ is shorter than T, a part or all of the echo will be lost because a monostatic radar cannot receive while the transmitter is still on. Hence D = cT/2 is called the eclipsing distance.

For a hypothetical moving point target, the echo will be a time delayed, Doppler shifted version of the transmitted pulse:

$$u_r(t) = A' \exp\{j2\pi[f_d + \frac{\mu(t-\tau)}{2}](t-\tau)\} \tag{7}$$

Where $f_d = \frac{2v}{\lambda}$ is the Doppler shift in Hz due to the velocity of the target, and λ is the radar wavelength. Since the carrier frequency varies linearly with time, the wavelength λ is also a function of time:

$$\lambda(t) = \frac{c}{(f_o + \mu t)} \tag{8}$$

For a narrow band linear FM signal the frequency sweep bandwidth is a small fraction of the carrier frequency. Consequently the variation in Doppler shift due to the frequency sweep may be neglected because the difference is small compared with the nominal Doppler shift at frequency f_o. For example, if f_o=10 GHz and B=10 MHz, the difference in Doppler shift due to the same target at the beginning and the end of the FM pulse is only 0.1%.

2.1.1 Processing of pulsed linear FM signals.

Optimal processing of radar signals requires a filter that is matched [3] to the transmitted waveform. In the time domain, the matched filtering operation may be realized by a correlation between the received waveform and the complex conjugate of the transmitted waveform. For the waveform in (7) we have:

$$M(\tau,f_d) = A\,A' \int_{-\infty}^{\infty} \exp\{j2\pi(f_d+\frac{\mu\, t}{2})t\} \exp\{-j\pi\mu(t-\tau)^2\}\, dt \qquad (9)$$

Referring to Figure 1, the waveform u(t) is the echo returned from a point target at an arbitrary range. Since the target range is arbitrary, there is no fixed reference with respect to the time–of–arrival of the echo. We may consider that the function u(t) begins at time $t = -T/2$ and ends at $t = T/2$. As τ increases the function $u^*(t-\tau)$ will be translated to the right on the time axis. For values of $\tau < -T$ and $\tau > T$, the two waveforms do not overlap. Hence the correlation is zero for these values of τ. From $\tau = -T$ up to $\tau = T$, the two waveforms overlap and the correlation becomes non–zero. For $-T \le \tau \le 0$, the region within which the two waveforms overlap is from $-T/2$ to $T/2+\tau$. For $0 < \tau \le T$, the overlap region is from $-T/2+\tau$ to $T/2$. Using these limits in the integration of (9) we have:

$$M(\tau,f_d) = k\,\mathrm{Rect}\left[\frac{\tau}{2T}\right]\exp(j\pi f_d\tau)\,\frac{T-|\tau|}{T}\,\frac{\sin[\pi(\mu\tau+f_d)(T-|\tau|)]}{[\pi(\mu\tau+f_d)(T-|\tau|)]} \qquad (10)$$

where $\mathrm{Rect}(\frac{t}{\delta}) = 1 \quad |t| \le \delta/2$

$= 0 \quad$ elsewhere,

and $k = A'AT$ is a constant of proportionality. The parameter k and the phase term $\exp(j\pi f_d\tau)$ are not important in so far as the magnitude of the response is concerned. The rectangular function Rect{ } is used to ensure that the response is zero for $|t| > T$.

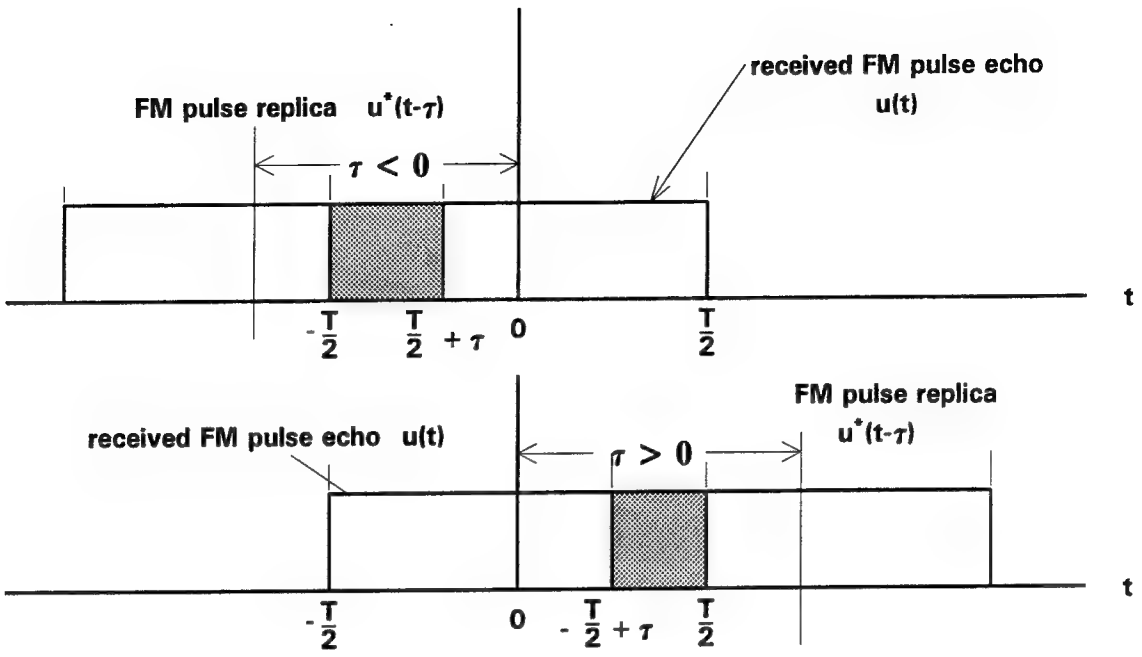

Figure 1. Integration limits for linear FM pulse compression.

2.1.2 Ambiguity function for a linear FM pulse.

Equation (10) represents a function of two variables, τ and f_d which is a surface in the 3–dimensional space of magnitude, time–delay and Doppler. A plot of this surface, normalized to the maximum response at (τ=0,f_d=0), is shown in Figure 2 for the following set of parameters: T = 10 μsec and B = 1 MHz.

The surface shown in Figure 2 is called the ambiguity function defined as the Fourier transform (with a change of sign in the exponential kernel) of the product of the transmitted pulse and its complex conjugate delayed by an amount τ:

$$\chi(\tau,\nu) = \int_{-\infty}^{\infty} u(t)\, u^{*}(t-\tau)\, \exp(j2\pi\nu t)\, dt \qquad (11)$$

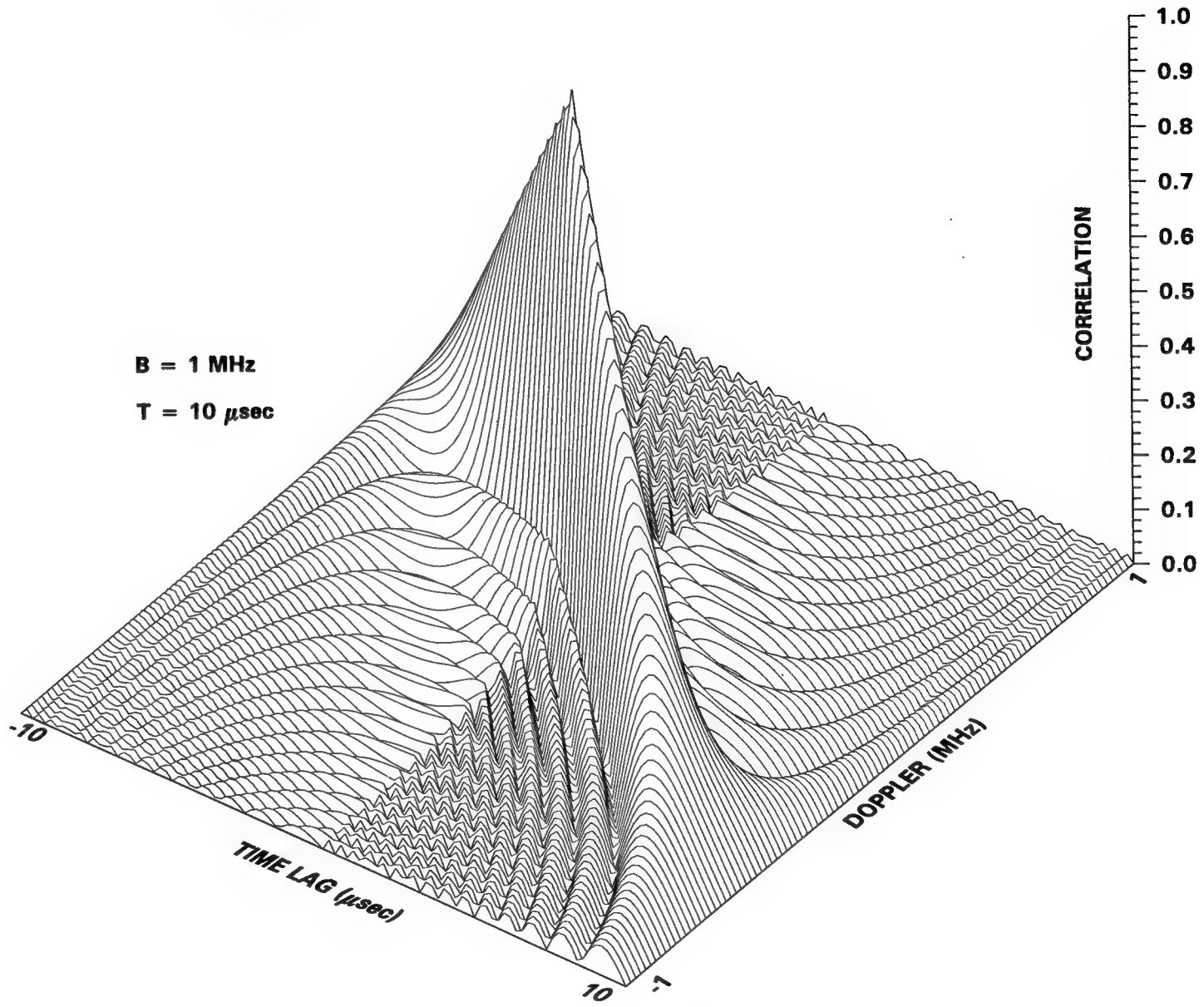

Figure 2. Ambiguous surface for a linear FM pulse.

It can be seen that (11) becomes (9) if we let $u(t)=\exp(j\pi\mu t^2)$, and $\nu = f_d$.

Range–Doppler ambiguity

Equation (10) represents the response of a filter that is matched to a target at some arbitrary range. Ideally the filter should match the target in both range and Doppler. By matching in range it is meant that an output sample is taken from the filter at precisely the time instant when the target echo from that particular range is expected to produce a maximum response. By taking samples from the matched filter output at regular time intervals, it is equivalent to sampling the output of a bank of filters matched to targets at different ranges. With respect to a given time instant, a target will have to be at a specific range and Doppler shift in order to produce a maximum response. This condition is represented by (τ=0, f_d=0). For targets that are not matched to the filter either in range or in Doppler, there will be a gradual deterioration of the correlation peak as the mismatch increases. In subsequent discussions, we shall assume that the matched filter is matched to a stationary target.

The intersection of the surface in Figure 2 with a vertical plane on which f_d is constant gives the response of the filter to targets with a constant velocity at various ranges. This is shown in Figure 3a for $f_d = 0$. The intersection of the surface in Figure 2 with a vertical plane on which τ is constant gives the response of the filter to a target at a fixed range but with various Doppler shifts. This is shown in Figure 3b for a value of $\tau = 0$. It can be seen that the filter response drops off rapidly as f_d deviates from 0.

The intersection of the surface in Figure 2 with the vertical plane that contains the line $\mu\tau+f_d = 0$ on the τ–f_d plane is shown in Figure 3c. It can be seen that the correlation decreases rather slowly. This means that a target at a range other than the one that the filter is matched to will produce a response that is only slightly weaker than the maximum response if the target's Doppler shift satisfies the condition $f_d + \mu\tau = 0$. Since there is no a priori information regarding either the location, the velocity or the magnitude of the target, one is not certain whether the response from the matched filter is a result of a stationary target at that location or a moving target at another location. This condition is referred to as "range–Doppler ambiguity".

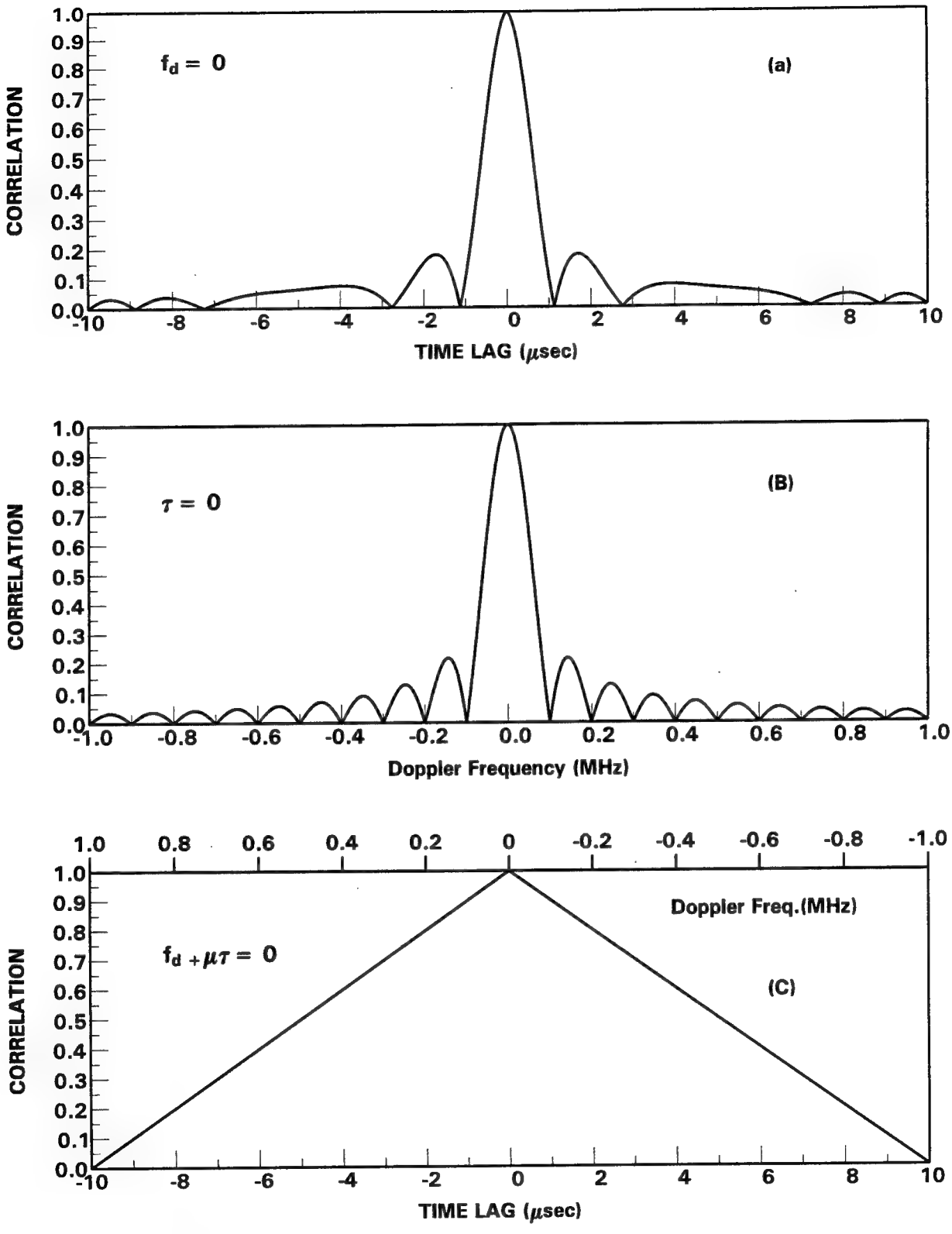

Figure 3. Matched filter responses: (a) Doppler-Matched, (b) Range-matched and (c) on plane of range-Doppler ambiguity

Pulse compression ratio and time–bandwidth product.

Consider the matched filter output response of (10) to a stationary target located at a distance corresponding to a time delay τ very close to the origin (i.e., $\tau \approx 0$, and $f_d = 0$). Under these conditions, (10) becomes:

$$\chi(\tau,0) \approx \frac{T-|\tau|}{T} \frac{\sin(\pi\mu\tau T)}{\pi\mu\tau T} = \frac{T-|\tau|}{T} \frac{\sin(\pi B\tau)}{\pi B\tau} \tag{12}$$

For small $|\tau|$, $T-|\tau|/T \approx 1$. we may write:

$$\chi(\tau,0) \approx \frac{\sin(\pi B\tau)}{\pi B\tau}. \tag{13}$$

At $\tau = 1/2B$, $\chi(\tau,0) \approx \sin(\pi/2)/(\pi/2) = 0.6366$ which is close to the half power point. The distance between the half power points (or the compressed pulse length) is in the order of $\Delta\tau = 1/B$. Hence the pulse compression ratio (the ratio between the uncompressed and compressed pulse lengths) is:

$$\rho = \frac{T}{(1/B)} = BT \tag{14}$$

which is the product between the transmit pulse length and the FM sweep bandwidth or simply the time–bandwidth product.

2.2 FMCW waveform.

In Section 2.1 we discussed some of the concepts pertinent to linear FM signals. The pulse–compression–ratio is approximately given by the time–bandwidth product. A given value of time–bandwidth product may be obtained in two ways: (i) a high frequency

sweep rate with a relatively short pulse length or (ii) a relatively low sweep rate with a long pulse length. Since the eclipsing distance is proportional to the uncompressed pulse length, it is not practical to transmit excessively long pulses if close–in ranges are of interest.

If, on the other hand, the radar operates in a bistatic mode, the transmitter and the receiver can be turned on simultaneously, and the echo signal can be received continuously. This assumes of course that there is sufficient isolation between the transmitter and the receiver so that there will not be excessive interference in the receiver by the transmitted signal (e.g., saturation of the receiver by the much stronger transmitted signal) Radars that transmit a sinusoidal signal over a long duration are generally referred to as CW radars.

When Linear FM is applied to the transmitted continuous sinusoidal signal, the resulting waveform is called an FMCW. The echo of an FMCW signal may be processed in an analogous manner as that in the FM pulse case (i.e., matched filter or correlation). Theoretically, if the frequency sweep is permitted to continue indefinitely, very fine range resolution can be obtained. In practice, the frequency of the signal cannot increase or decrease indefinitely. Consequently the carrier frequency is a piece–wise linear function of time. An FMCW signal is represented in complex exponential form as:

$$s(t) = A \exp\{j2\pi[f_n + \frac{\mu_n (t - nT_s)}{2}](t - nT_s)\} \qquad (15)$$

$$nT_s \leq t \leq (n+1)T_s \qquad n=0,1,2,....$$
$$|\mu_n| = \mu > 0$$

At time instants $t = nT_s$, the way the carrier frequency is being swept will be changed. One has the choices of either changing the frequency back to $f_n = f_0$ and resume the frequency sweep as before, or changing the sign of μ_n (i.e., changing from a positive to a negative frequency sweep and vice versa). If the carrier frequency is changed back to f_0 at the beginning of each period $t=nT_s$, it results in a saw–tooth waveform for the carrier frequency as depicted in Figure 4a. If the sign of μ_n is reversed at $t=nT_s$ while the carrier frequency remains continuous, a triangular waveform for the carrier frequency results as depicted in Figure 4b.

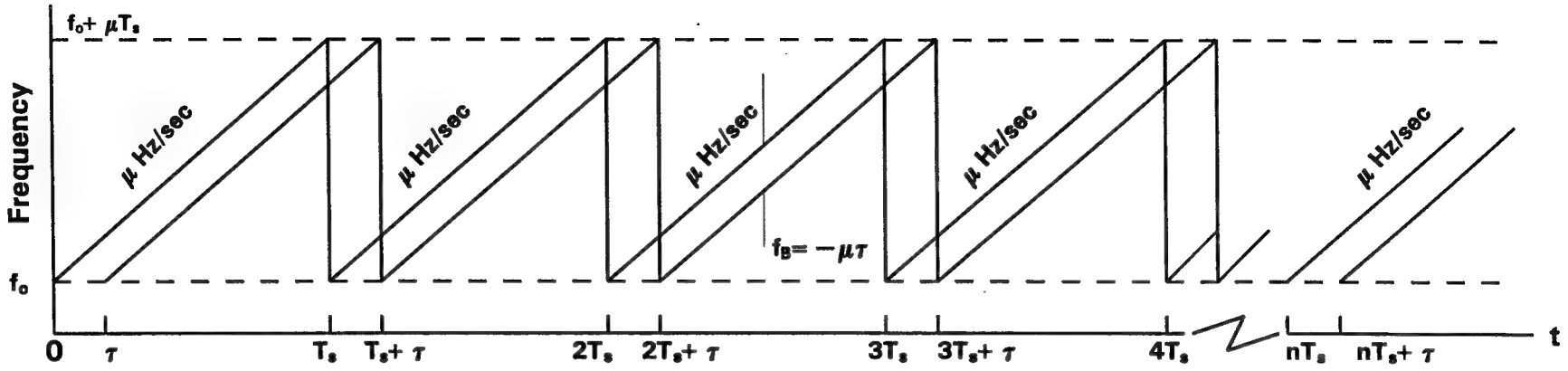

(a) Saw-tooth variation of carrier frequency.

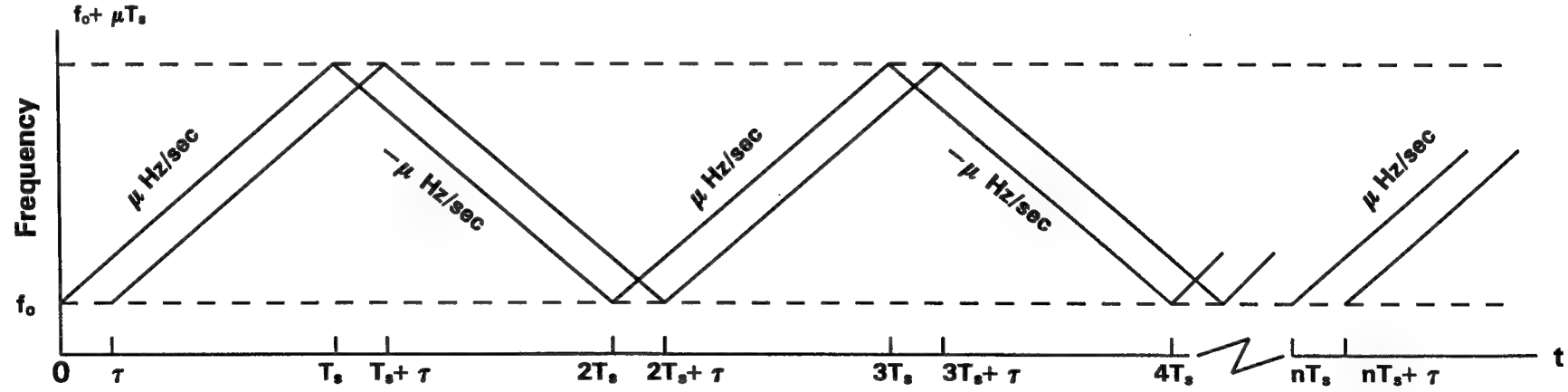

(b) Triangular variation of carrier frequency.

Figure 4. Alternative ways of frequency variation for FMCW waveform.

2.2.1 Processing of the FMCW waveform.

The optimal processing of FMCW signals depends on several factors: (a) the way the carrier frequency sweep is switched, (b) whether coherence can be maintained between successive sweeps and (c) whether there is a significant amount of Doppler shift in the target echo. In the following we shall discuss the conventional way of processing the FMCW signal. We consider a saw–tooth variation of the carrier frequency and assume that there is a short time interval between successive sweeps for the transmitter to reset parameters. Consequently, the processing utilizes the data in a single sweep only. The transmit waveform is given by:

$$s(t) = A \exp\{j2\pi(f_o + \frac{\mu t}{2})t\} \qquad 0 \le t \le T_s \tag{16}$$

A point target located at range R and travelling at a velocity v will return an echo:

$$s'(t') = A' \exp\{j2\pi(f_o + f_d + \frac{\mu t'}{2})t'\} \tag{17}$$

where $t' = t - \tau$, $\tau = 2R/c$ and $f_d = 2vf_o/c$.

This signal is mixed with a reference signal synchronized to the transmit signal which at time t' will be:

$$s(t') = A \exp\{-j2\pi(f_o + \frac{\mu(t'+\tau)}{2})(t'+\tau)\} \tag{18}$$

The result is:

$$m(t') = A'A \exp\{j2\pi[(f_d - \mu\tau)t' - (f_o + \frac{\mu\tau}{2})\tau]\} \qquad \tau \le t' \le T_s \tag{19}$$

Equation (19) is recognized as a complex sinusoidal signal with a constant frequency ($f_d - \mu\tau$). For stationary targets ($f_d = 0$), the matched filter is a correlator comprising a set of complex sinusoids that are the conjugate of the waveforms $\exp(-j2\pi\mu\tau t)$, that is $\exp(j2\pi\mu\tau' t)$. The frequency of the sinusoids is called the "beat frequency":

$$f_B = -\mu\tau. \tag{20}$$

between the reference signal and the returned echo from a given range corresponding to a round–trip delay of τ. From (6) and (20) the target range can be determined from the beat frequency:

$$R = \frac{cf_B}{2\mu} \tag{21}$$

The output of the correlator is:

$$M(\tau', f_d, \tau) = A'A \int_{-\infty}^{\infty} \exp\{j2\pi[(f_d - \mu\tau)t - (f_o + \frac{\mu\tau^2}{2})]\} \exp\{j2\pi\mu\tau' t\}\, dt$$

$$= A'A \exp\{-j2\pi(f_o + \frac{\mu\tau}{2})\tau\} \frac{\exp\{j2\pi[f_d + \mu(\tau' - \tau)t]\}}{j2\pi[f_d + \mu(\tau' - \tau)]}\Bigg]_{-T_s/2+\tau}^{T_s/2}$$

$$= A'A \exp\{-j2\pi(f_o + \frac{\mu\tau}{2})\tau\} \times \tag{22}$$

$$\frac{\exp\{j2\pi[f_d + \mu(\tau' - \tau)](T_s/2)\} - \exp\{j2\pi[f_d + \mu(\tau' - \tau)](-T_s/2 + \tau)\}}{j2\pi[f_d + \mu(\tau' - \tau)]}$$

$$= k \exp\{-j2\pi(f_o + \frac{f_d + \mu\tau'}{2})\tau\} \frac{T_s - \tau}{T_s} \frac{\sin\{\pi[f_d + \mu(\tau' - \tau)](T_s - \tau)\}}{\pi[f_d + \mu(\tau' - \tau)](T_s - \tau)}$$

where $k = A'AT_s$.

Equation (22) is the Fourier transform (except for the change of sign in the exponential $\exp\{j2\pi\mu\tau' t\}$) of the mixer output described in (19). The correlator output also depends on the target range, as indicated by the presence of parameter τ. This is a consequence of the fact that, as the target range increases, the portion of the echo waveform that can be transformed is proportionately reduced by a factor $(T_s-\tau)/T_s$. Since the FM sweep period is T_s seconds, the frequency resolution of the transform is:

$$\Delta F = 1/T_s \tag{23}$$

and the range resolution of the FMCW is:

$$\Delta R = \frac{c}{2\mu T_s} \tag{24}$$

2.2.2 Ambiguity surface for FMCW.

Equation (22) is the ambiguity function for the FMCW waveform that employs a uni–directional frequency sweep (i.e., the carrier frequency is swept in the same manner in each FM sweep period, either upward or downward). It is similar to that of the linear FM pulse. Like the ambiguity function for the linear FM pulse, it is also a function of Doppler shifts. However, for most applications involving FMCW waveform, the Doppler shift is so small that it suffices to consider the response at zero–Doppler. We shall call (22) with $f_d = 0$ the range transform of an FMCW waveform because each frequency of the transform corresponds to a unique range through (20), assuming a stationary target.

One of the applications for the FMCW waveform is the radar altimeter [7]. In this case the target is stationary (the ground) and the target range of interest is very close to the radar. This permits the use of relatively long FM sweep periods to yield very fine altitude resolution.

2.3 FMICW Waveform.

Sometimes it is not practical to employ separate transmitter and receiver that are co–located and operate them continuously. This could be because of the difficulties in achieving a sufficiently high degree of isolation between the transmitter and the receiver. On the other hand, it may also be impractical to employ conventional pulsed FM signals because of the limitation on the instantaneous bandwidth of the transmitter and receiver. A low FM sweep rate must be employed. In other words, the carrier frequency must be swept over a much longer period to achieve the required time–bandwidth product. This means that the eclipsing range would be unacceptably large. Sometimes the required length of the FM sweep period is so great that the eclipsing distance extends to tens of thousands of km, thereby rendering it useless for radar application. For example, if it is required to sweep the carrier frequency over a period of 0.5 seconds, the eclipsing range is $cT_s/2 = 0.75 \times 10^8$ m.

The FMICW is a modification of the FMCW designed to permit monostatic radar operation while retaining some of the advantages of an FMCW system. Figure 5a shows the timing diagram for the carrier frequency of an FMICW radar over two FM sweep periods. Pulses of a linear FM waveform of duration τ_p are transmitted at regular intervals of T_f as shown in figure 5b. The frequency variation of the pulse emitted at time $t = nT_f$, $n = 0,1,2,...,N-1$, is shown in Figure 5a at the corresponding location on the time axis (i.e., the line segments bounded by the two short vertical lines about $t = nT_f$).

In one FM sweep period T_s, the FMICW signal is represented mathematically as:

$$s(t) = \sum_{n=0}^{N_p-1} \text{Rect}\left[\frac{t-nT_f}{\tau_p}\right] \exp\{j2\pi[f_0 t+\frac{\mu t^2}{2}]\} \qquad (25)$$

where T_f is the radar pulse repetition interval (PRI), τ_p is the pulse length and N_p is the number of pulses transmitted in an FM sweep period T_s.

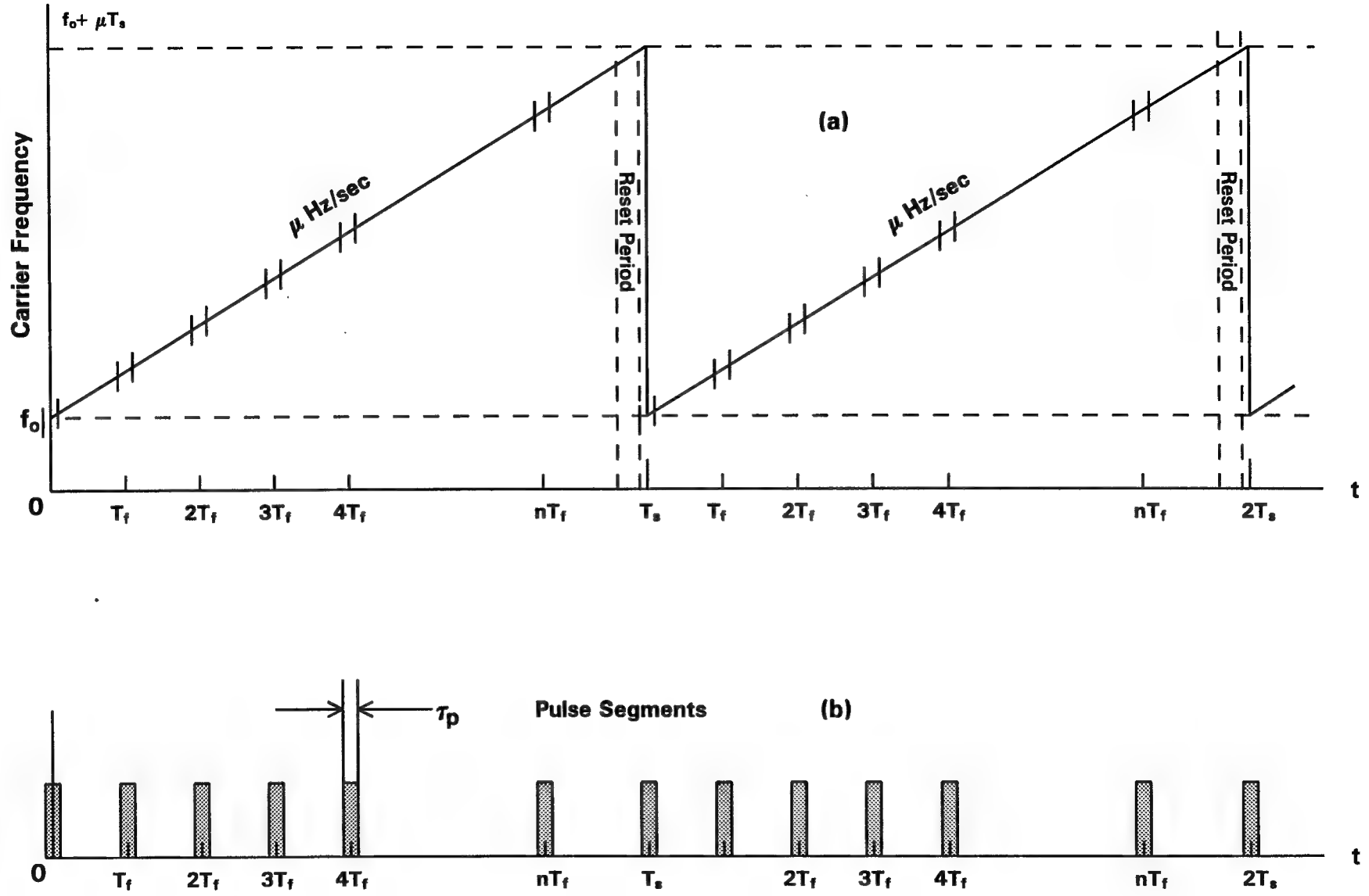

Figure 5. FMICW pulse train: (a) Carrier frequency variation and (b) Pulse timing.

The signal in (25) is nothing more than an FMCW waveform gated by a rectangular pulse train with pulse width τ_p and a period of T_f. We call the set of pulses emitted at time instants $t = nT_f$ "pulse segments" to distinguish them from the conventional FM pulses because the FMICW pulses are segments of a complete FMCW waveform. The carrier frequency of the signal at time $t = nT_f$ is governed by the relationship:

$$f_n = f_o + \mu n T_f \tag{26}$$

$$n = 0,1,2,...,N_p-1.$$

and the phase of the signal at time $t=nT_f$ relative to that at the beginning of the FM sweep period is given by:

$$\phi_n = 2\pi(f_o + \frac{\mu(nT_f)}{2})(nT_f). \tag{27}$$

Since T_f is the PRI of the radar, there can be a maximum of $N_p = T_s/T_f$ pulse segments in an FM sweep period T_s. The receiver is turned on in the time interval beginning immediately after each pulse transmission and ending at the time instant of the transmission of the next pulse. The receiver will be able to receive the complete echo of the transmitted pulse produced by a target whose round trip delay τ is greater than τ_p but less than $T_f-\tau_p$. After each FM sweep period, there will be a short time interval for the transmitter to reset parameters. The carrier frequency will return to the initial value of f_o, and the entire sequence of transmission repeats itself.

The echo signal returned from a point target, located at a range corresponding to a round–trip delay of τ, to an FMICW signal (ignoring the amplitude scaling) is given by:

$$s_r(t') = \sum_{n=0}^{N_p-1} \text{Rect}\left[\frac{t'-nT_f}{\tau_p}\right] \exp\{j[2\pi(f_o+f_d)t'+\pi\mu t'^2]\} \tag{28}$$

where $t' = t-\tau$, and f_d is the Doppler shift of the target.

To process the FMICW echo waveform, the signal of (28) is first mixed with the reference signal in (26) yielding (the prime is dropped to simplify the notation):

$$m(t) = \sum_{n=0}^{N_p-1} \text{Rect}\left[\frac{t-nT_f}{\tau_p}\right] \exp\{j[2\pi(f_o+f_d)t+\pi\mu t^2]\} \times \exp\{-j[2\pi(f_o+\frac{\mu(t+\tau)}{2})(t+\tau)]\} \quad (29)$$

$$= \sum_{n=0}^{N_p-1} \text{Rect}\left[\frac{t-nT_f}{\tau_p}\right] \exp\{j[2\pi(f_d-\mu\tau)t - (f_o+\mu\tau)\tau]\}$$

Equation (29) represents a gated complex sinusoidal signal with a constant frequency $(f_d-\mu\tau)$ Hz. In the next two sub–sections, we will discuss the signal processing procedure necessary to extract the range information from the returns of an FMICW signal.

2.3.1 Conventional signal processing for the FMICW.

When an FMICW pulse segment is transmitted, echoes will be returned from all the objects located at various ranges. The composite return of an FMICW signal is a superposition of these echoes. This situation is depicted in Figure 6a and 6b for a number of transmitted pulse segments. Because the returned signal is mixed with the reference signal whose frequency varies linearly with time, the mixer output signal will be composed of echo segments whose frequency increases linearly with time. This will be the case if all the objects are stationary, which we shall assume for the moment.

The FM sweep rate for the next pulse segment is identical to that of the preceding one, except that the sweep commences at a higher frequency determined by (26). But because the frequency of the reference signal also varies at the same rate μ, essentially the same composite waveform will be obtained from the next pulse segment. Furthermore, the echo segments of the returned signal from successive pulse segments are phase coherent because the reference signal and the transmitted signal remain coherent from pulse to pulse.

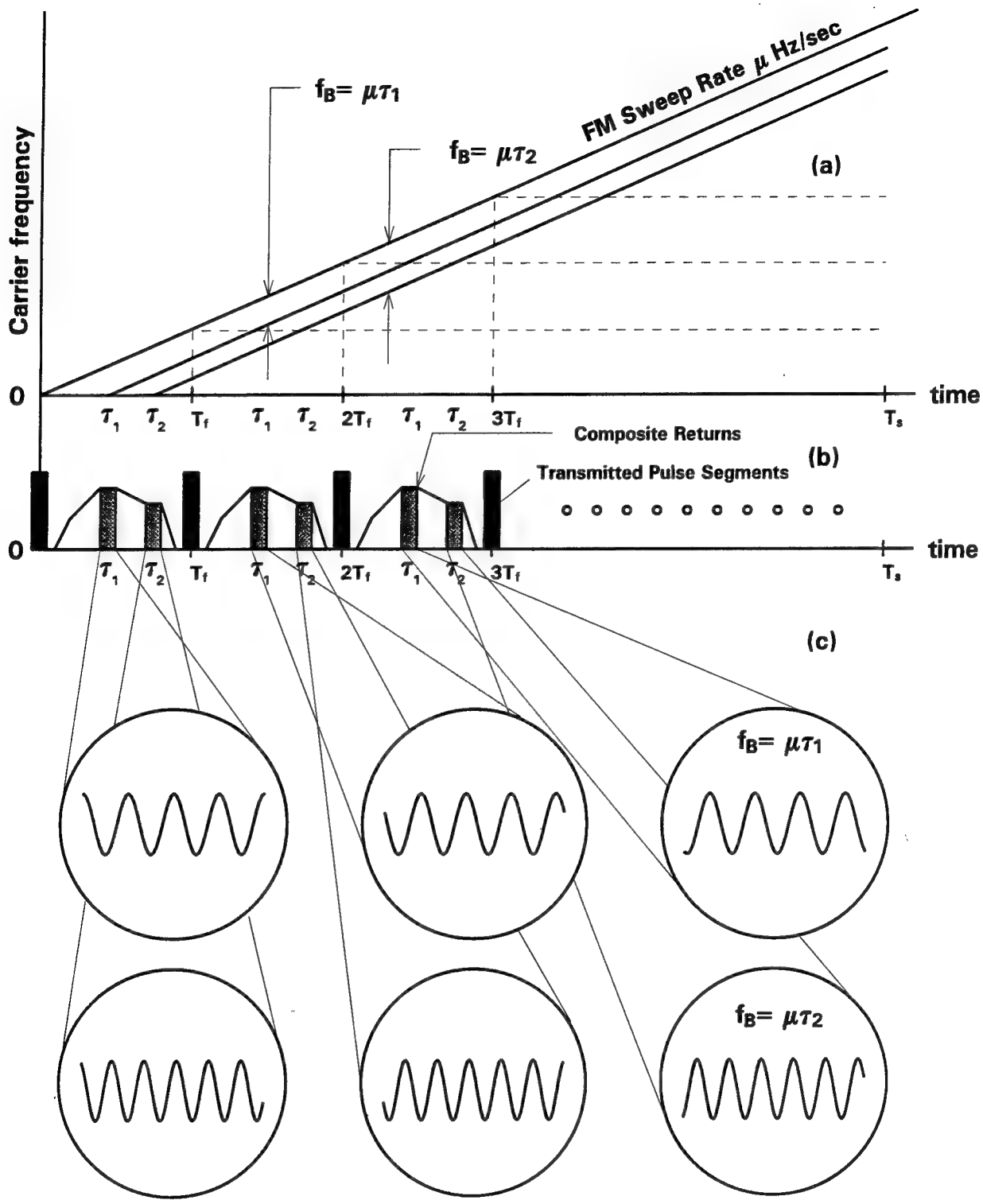

Figure 6. Operation of the FMICW: (a) Carrier frequency variation, (b) Composite returns and (c) Echo waveforms.

In Figure 6b we isolate two contiguous segments of the returned waveform that correspond to two separate point targets located at a range $R_1=c\tau_1/2$ and $R_2 = c\tau_2/2$, respectively, for each transmitted pulse segment. These echo segments are magnified and shown in Figure 6c. It shows that the beat frequency for the target located at R_2 is higher than that for the target at R_1. The beat frequency for the waveform segment corresponding to a fixed range, however, remains constant from one pulse to the another. The echo segments from the same range are continuous from one pulse segment to the next if data were available. That is, if a particular echo segment from the preceding transmitted pulse segment were permitted to continue in time, by the time the echo due to the next pulse from the same target arrives, it will match the waveform in phase as if it has not been interrupted.

It should be pointed out that the illustration of Figure 6c has been exaggerated. In reality, the sinusoidal waveform segments will likely be composed of a fraction of a cycle. The waveforms are shown in multiple cycles because it would be difficult to tell which of the two sine waves has a higher frequency with only a fraction of a cycle shown.

The mixer output is sampled at a rate at least equal to the Nyquist rate [8] and digitally demodulated down to complex baseband (i.e., I– and Q–channel samples). The result, after the sampled returns from all N_p pulse segments are collected, is a time series with gaps that contain samples with the value of zero. These gaps correspond to the time intervals in which the transmitter is on.

A straightforward way of processing this time series would be to perform a Discrete Fourier transform (DFT) on it. The fast Fourier transform (FFT) algorithm [9] is an efficient method for computing the DFT which can be interpreted as a bank of complex correlators correlating the time sequence $\{x_n\}$ with a set of N sampled sinusoids. This is obvious from the definition of the DFT:

$$F_k = \frac{1}{N} \sum_{n=0}^{N-1} x_n \exp\{-j\frac{2\pi nk}{N}\}. \qquad (30)$$

$$k = 0,1,2,\ldots,N-1$$

The frequency of the kth correlator bin is given by $k\Delta F$ where $\Delta F = f_s/N$ and f_s is the sampling frequency of the time series. The correlation is over the entire sequence from x_0 to x_{N-1}.

For very long time series, the computational effort required by the FFT is only a fraction of that required for the direct calculation of the DFT. Take, for instance, the number of required multiplications. An N–point DFT would require N^2 complex multiplications. On the other hand, an FFT implemented with the Radix–2 algorithm [10] requires about $N \log_2 N$ complex multiplications. For a 65536–point FFT ($\log_2 N=16$), the reduction in the number of multiplications is 99.98%.

For the purpose of processing the FMICW data, however, this saving in computational effort is less significant than first appears. The reasons are as follows. First, an FFT computes the spectral components of the input sequence at a number of discrete frequencies, regardless whether they are required or not. For a radar employing FMICW, the spectral output (which will be called spectral bins) of interest is confined to a small fraction of the total number of bins. Using the DFT one needs to compute the required frequency bins only. Thus the saving in computational effort of the FFT over that of the DFT is actually much less.

Second, if the time series contains a significant portion that is composed of contiguous zeros, the FFT will still perform the multiplications and additions. A shorter correlator may be employed equally well to perform the calculation on the portion of the time series that have non–zero values and combine the results afterward to yield the complete DFT of the time series. This approach will be used in the modified processing scheme to be described in Section 2.3.2. For a straightforward processing of the composite returns, the FFT approach is still more efficient and will be used.

By performing an FFT on the sampled signal of (29), stationary targets located at a particular range cell will be indicated by a larger than usual magnitude at a frequency bin determined by:

$$f_B = \frac{2\mu R}{c} \tag{31}$$

where R is the target range.

Conversely the range of the target detected from a particular frequency bin f_B is determined by (21).

The frequency bins of the FFT that are of interest are the ones with frequencies less than (or greater than if $\mu < 0$) or equal to the beat frequency resulted from a target at the maximum unambiguous range:

$$f_{max} = \mu T_f \tag{32}$$

2.3.2 Problems encountered in the conventional FMICW processing procedure.

The processing scheme described above results in two problems which will be discussed in what follows.

(a) Ambiguous Range Response.

Unlike the FMCW waveform, the time series of the returned FMICW signal from a single target is not continuous because the transmit waveform is a pulse train. We may consider equivalently that the time series is continuous but that it is being multiplied by a gating function defined as:

$$G(t) = \sum_{n=0}^{N-1} \text{Rect}\left[\frac{t - nT_f}{\tau_p}\right] \tag{33}$$

where $\text{Rect}\{\frac{t}{T}\} = 1 \quad |t| \le \frac{T}{2}$

$= 0 \quad$ elsewhere

To visualize what happens to the correlator output when the input of a continuous signal is interrupted periodically, we may consider the Fourier transform of a complex sinusoid gated by a rectangular pulse train of width τ_p and period T_f:

$$s(t) = \exp\{j2\pi f_o t\} \sum_{n=0}^{N-1} \mathrm{Rect}\left(\frac{t-nT_f}{\tau_p}\right) \tag{34}$$

A sinusoidal function, the gating function of (33) and the product of the two are shown in Figure 7a, 7b and 7c, respectively.

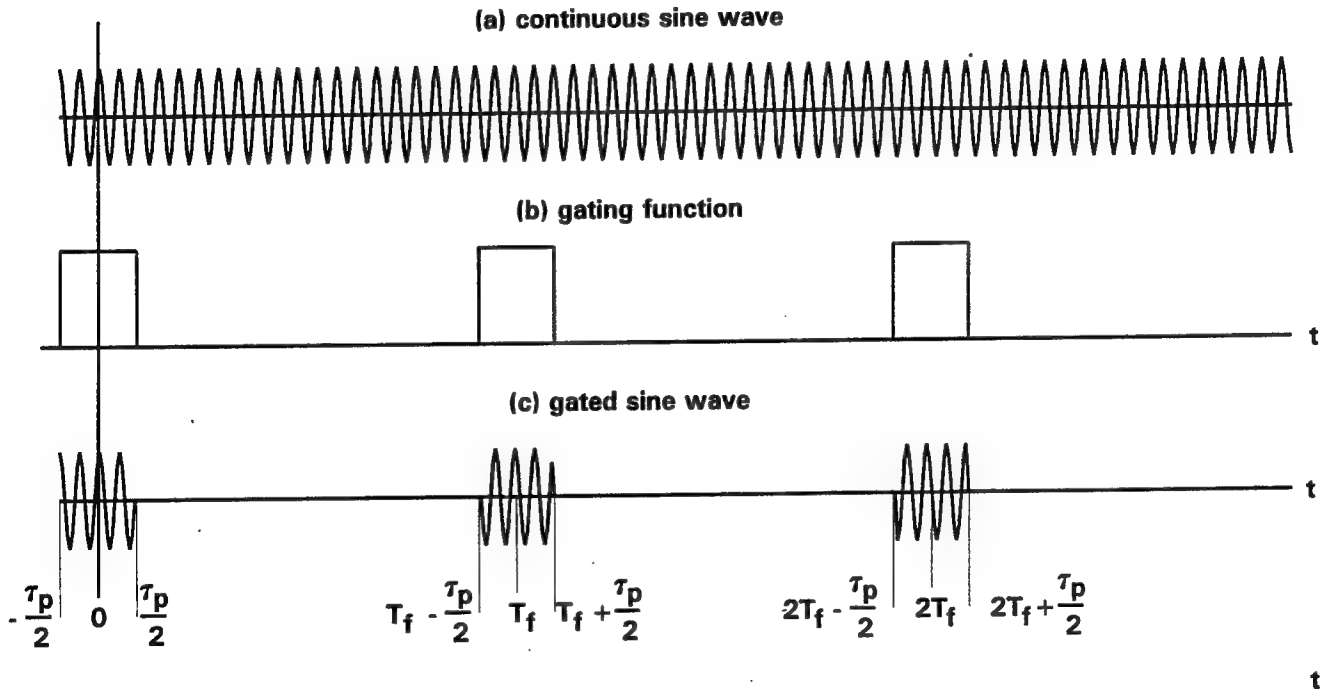

Figure 7. A gated sinusoidal waveform.

The Fourier transform of (34) may be obtained by performing the integration directly:

$$S(f) = \int_{-\infty}^{\infty} \exp\{-j2\pi(f-f_o)t\} \sum_{n=0}^{N-1} \mathrm{Rect}\left(\frac{t-nT_f}{\tau_p}\right) dt. \tag{35}$$

Interchanging the order of integration and summation yields:

$$S(f) = \sum_{n=0}^{N-1} \int_{-\infty}^{\infty} \mathrm{Rect}\left(\frac{t-nT_f}{\tau_p}\right) \exp\{-j2\pi(f-f_o)t\}\, dt.$$

$$= \sum_{n=0}^{N-1} \int_{nT_f-\tau_p}^{nT_f+\tau_p} \exp\{-j2\pi(f-f_o)t\}\, dt \tag{36}$$

$$= \frac{\sin[\pi(f-f_o)\tau_p]}{\pi(f-f_o)\tau_p} \sum_{n=0}^{N-1} \exp\{-j2\pi(f-f_o)nT_f\}$$

Let us examine the summation in (36). The complex exponentials in the summation will all have a value of unity whenever $(f-f_o)T_f = k$ (or when $f = f_o+k/T_f$; k is an arbitrary integer) yielding a value of N for the summation. The sum decreases rapidly as f deviates from f_o+k/T_f. It can be seen that the Fourier transform of a sinusoidal signal gated by a rectangular pulse train has a periodic spectrum. The principal spectrum which is centered at the frequency $f=f_o$ replicates itself along the frequency axis with a period of $1/T_f$ Hz. The magnitude of the spectral replicas is scaled according to an envelope $\sin\{\pi(f-f_o)\tau_p\}/[\pi(f-f_o)\tau_p]$.

Since there is a direct relationship between the frequency of the correlator bin and the target range, a target located at some arbitrary range R will also produce responses at other ranges $R' = R \pm nR_a$, $n = 1,2,...$, where

$$R_a = \frac{c}{2\mu T_f} \tag{37}$$

This is known as the ambiguous range response. This ambiguous range response is not to be confused with the ambiguous range associated with targets at long ranges appearing as close–in targets on account of their having a round–trip delay greater than the radar PRI. The ambiguity referred to here is a consequence of the periodicity of the interrupted sequence which in effect produces strong correlation between the input and sinusoidal replicas whose frequency is related to the frequency of the input sequence by:

$$f_a = f + \frac{k}{T_f} \tag{38}$$

where f is the frequency of the interrupted sinusoidal sequence, T_f is the interrupt period and k is an arbitrary integer.

Figure 8 shows the magnitude of the FFT of an interrupted complex sinusoidal time series with a beat frequency of 900 Hz. The sampling interval is 8 μsec, and the interrupt period is 3 msec. The time series is composed of blocks of 30 samples (240 μsec) of the complex sinusoid separated by blocks of 345 zeros. The first non–zero segment begins at the 150th samples. This time series is what would be expected from a stationary point target located at a range of 180 km from an HFSWR transmitting an FMICW waveform with the following characteristics:

$\mu = 750$ kHz/sec.
$T_f = 3$ msec
$\tau_p = 240$ μsec
$T_s = 0.524288$ sec.

It can be seen that there is a maximum response at the frequency bin of 900 Hz. But there are also strong responses at frequency bins which differ from 900 Hz by an integer multiple of $1/T_f$ (333.33 Hz). The relative magnitudes of the periodic responses follow a sin(x)/x envelope as predicted by theory. The spectral line at 900 Hz is the true response, while the other spectral lines are the ambigouous responses. From (37), the distance corresponding to the spectral period (or the ambiguous range) is $R_a = \frac{c}{2\mu T_f} =$ 66.67 km.

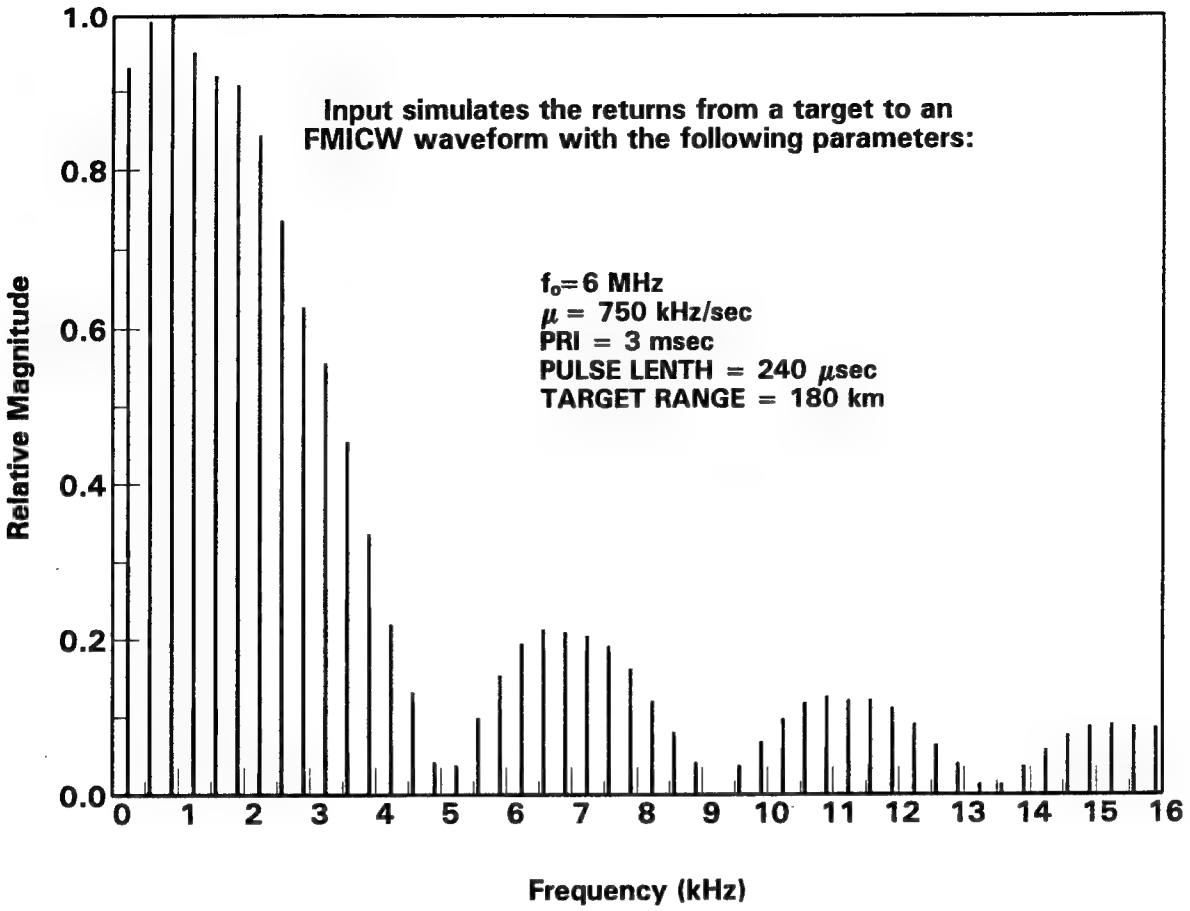

Figure 8. Fourier transform of an interrupted sinusoid.

(b) Masking of targets at long range by those at close–in ranges.

As a consequence of the ambiguous range response discussed in Section 2.3.1a, a further complication arises pertaining to the masking of targets at longer ranges by those at close–in ranges. This effect is discussed in [11]. The radar echoes are subjected to the normal R^{-4} attenuation due to the two–way spherical dispersion of the radar signal. For HFSWR there is a further attenuation of the radar signal due to the surface wave attenuation factor. This means that a target located at range R could produce a larger response at range $R+R_a$ than it would if it were actually located there.

Since there is no a priori information on the location of targets, it is difficult to determine whether there is a target at one of the two locations or both. These are problems associated with FMICW that must be addressed. In Section 2.4 we shall present a modified processing scheme for FMICW that circumvents both of these problems.

2.4 A modified FMICW processing scheme.

To alleviate the two problems associated with the conventional FMICW processing scheme, an alternative processing scheme needs to be developed that provides a means to determine the true target range from the ambiguous range. The rationale for developing the modified processing procedure in this report is to gain some understanding of the optimum processing of the FMICW waveform, its advantages and limitations. This background information is essential for the realistic assessment of the performance of the waveform against that of other waveforms. It is not the purpose of this work to perfect the signal processing procedure to the extent that it can be applied directly in an operational system. For example, no waveform shaping will be employed to suppress range sidelobes which would have to be investigated in an operational system.

As pointed out by Dr. Khan of C–CORE (Centre for Cold Ocean Research and Engineering), the various frequency components of the returned echo of an FMICW pulse segment do not arrive at the receiver's mixer output simultaneously. This is obvious from (20) which says that the frequency of the signal components of an FMICW echo at the output of the mixer is directly proportional to the time–of–arrival of the component. This fact can be used advantageously to develop an improved processing scheme for FMICW signals. The procedure described below performs the same function as the one developed by Dr. Khan; however, the details are believed to be different.

2.4.1 Modified FMICW processing procedure

Refer to Figure 9a which shows the composite returns of an FMICW pulse train over one FM sweep period. The returned waveform has been sampled at a rate of f_s samples/sec. Assume for the moment that the composite returns over one complete FM sweep period comprise the echoes from a number of M_s point targets only. These M_s targets are distributed over the unambiguous range ($cT_f/2$) with an equal spacing of $c\tau_p/2$ meters (the extent of the uncompressed range cell).

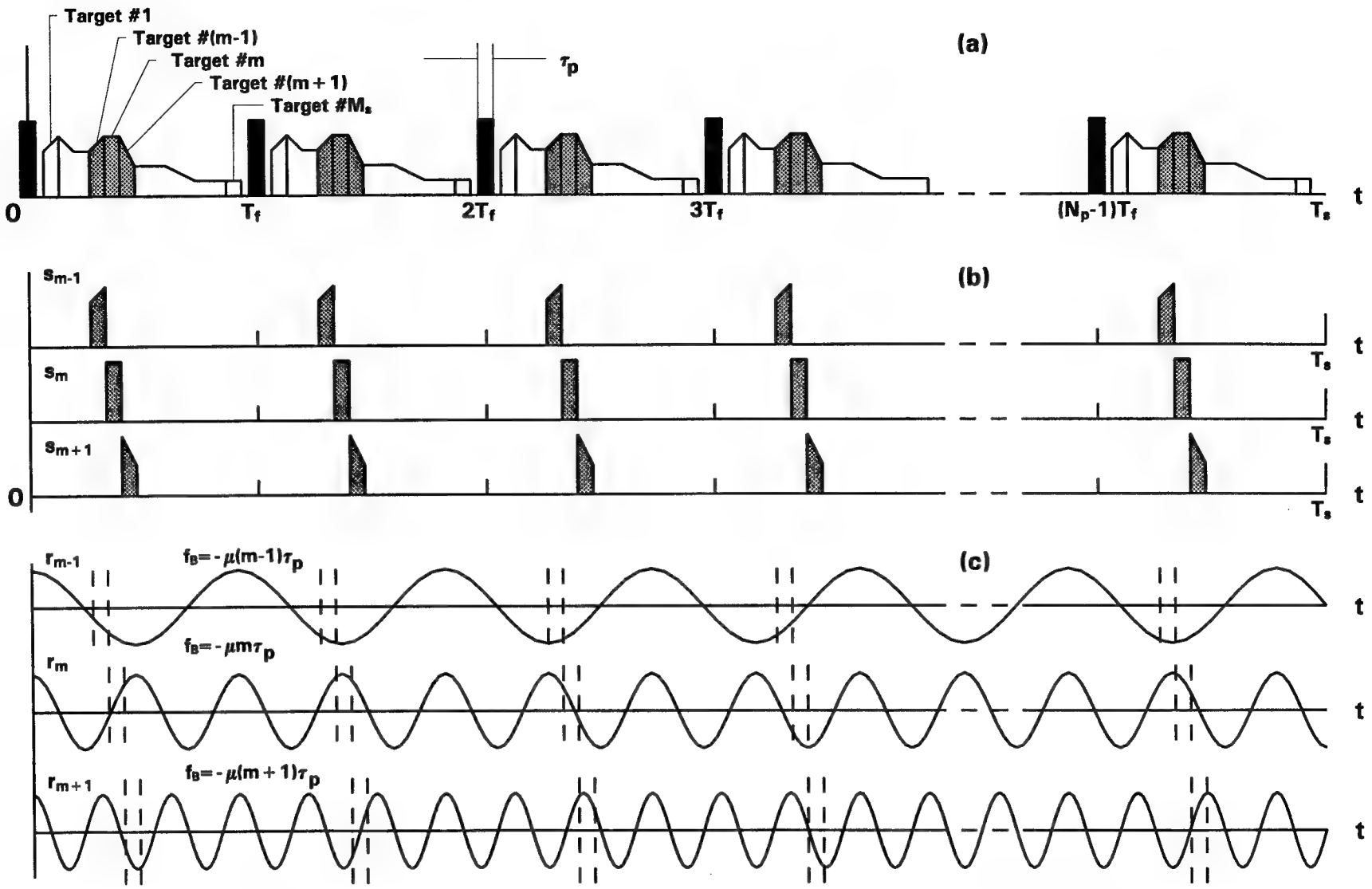

Figure 9. Operation of the modified FMICW processing scheme: (a) Composite return (b) Decomposed sub-sequences and (c) Correlator replicas.

The first target (i.e., the one closest to the radar) is located at a distance $R_1 = c\tau_p/2$. We shall number them from m=1 to M_s. If we consider the first uncompressed range cell begins at the range R_1 (the eclipsing range), the M_s targets are located at the near–end of each of the M_s uncompressed range cells.

Since a point target reflects an echo that is a scaled replica of the transmitted waveform, the echoes from each point target will last τ_p also. Here we are assuming that the receiver bandwidth is sufficiently wide so that the above condition is met. Consequently, the composite return will comprise contiguous blocks of sinusoidal waveforms of length τ_p and of increasing frequency given by $\mu m\tau_p$ (see (20)), where m indicates the mth target from the radar. Since the composite return is sampled at a rate of f_s samples/sec, each block will contain

$$N_s = \tau_p f_s \tag{39}$$

samples.

Next we decompose the composite time series into M_s mutually exclusive sub–sequences. Each sub–sequence is formed by retaining samples that corresponds to one of the M_s uncompressed range cells only. Since there is only one target in each uncompressed range cell, these decomposed time series correspond to the echoes from individual targets over one FM sweep period.

This scenario is depicted in Figure 9b. Three mutually exclusive subsequences designated as s_{m-1}, s_m and s_{m+1} are shown for the (m–1)st, the mth and the (m+1)st targets, respectively. Since the location of each target is known, the frequency of each sub–sequence can be determined from (20). The subsequence corresponding to the mth target will have a maximum correlation with a sinusoidal sequence whose frequency is $m\mu\tau_p$. The sinusoidal sequences that yield the maximum correlation with s_{m-1}, s_m and s_{m+1} are shown in Figure 9c as r_{m-1}, r_m and r_{m+1}, respectively. The correlation between the r_i and s_j will be low for $i \neq j$ because the frequencies of these sinusoids are harmonically related and consequently orthogonal to one another.

Notice that the sub–sequences s_m, m=1,2,..,M_s contain mostly zeros. Consequently, it suffices to perform the correlation calculation on the non–zero samples only. For each non–zero segment, the correlator replicas require only N_s samples taken from the sequences r_j, j=1,2,..,M_s. The segments of the sinusoid that will be used as correlator replicas are the regions between the vertical dashed lines intersecting the sinusoids of Figure 9c. It can be seen that although the replica samples for each decomposed sequence are obtained from the same sinusoidal function, they are not identical from one pulse segment to the next. The proper values for the replica samples will be discussed when we present the modified procedure for processing FMICW.

We can now consider how one may determine the presence of a target without ambiguity from the composite returns of an FMICW waveform. We do not know if there are any targets except that, if there are, they must be at one of the prescribed locations $R_m = mc\tau_p/2$.

Given the above we can decompose the composite returns into M_s mutually exclusive sub–sequences as described in the preceding paragraph and correlate each of them with the particular sampled sinusoidal sequence that is expected to yield a maximum correlation if a target is present at that range. Since by decomposing the composite returns into mutually exclusive sub–sequences, we know a priori that no samples corresponding to a target that is at a distance greater than $c\tau_p/2$ m from the one in question is included, we can be certain that a large correlation response can only be resulted from a target that is located at that range and not from targets at any of the ambiguous ranges. Consequently the problems of ambiguous range response are circumvented.

The scenario described above is a contrived one. In general the targets can be located anywhere inside an uncompressed range cell and, therefore, could be displaced by some arbitrary distance from the locations prescribed above. When this happens, two things result. The first is that the echo samples arising from this target will be split and become a part of two neighbouring sub–sequences (range–mismatch). The result is a reduction in the number of samples that can be used for the correlation. The second is that the frequency of the samples will not match exactly that of the sinusoid–replica samples. An additional complication arises if the target is non–stationary. The Doppler shift due to the velocity of the target will change the apparent beat frequency of the return, thereby producing an additional frequency–mismatch between the returned echo and the correlator replica. All of the above will result in a reduction of the correlation magnitude.

Let us consider the problem of frequency–mismatch first. A straightforward way to overcome this problem is to determine the range of the frequency–mismatch and utilize a bank of correlators, each with a frequency slightly displaced from the nominal frequency so that it will match that frequency produced by the displaced (or moving) target.

Since the time duration of the uncompressed pulse is τ_p, the difference in beat frequency produced by a target that is located at one end of an uncompressed range cell to that located at the other is $\mu\tau_p$. Additional increase or decrease in beat frequency may result from the Doppler shift of moving targets. Thus for each uncompressed range cell, we need a number of correlators with frequencies that will cover the frequency range:

$$F = \mu\tau_p + 2f_{dmax} \tag{40}$$

where f_{dmax} = the absolute value of the maximum anticipated target Doppler, and the factor of 2 is used to account for both approaching and receding targets.

A remaining parameter is the necessary number of correlators to be used. Since there is no need to use more correlators than are required to resolve targets that are one compressed range cell apart, an appropriate number of correlator is L:

$$L = \frac{\mu\tau_p + 2f_{dmax}}{\Delta F} \tag{41}$$

where $\Delta F = \frac{1}{T_s}$ is the resolution of the range transform as defined in (23).

Further consideration regarding the number of correlators for each uncompressed range cell will be discussed next when we present the modified processing procedure for FMICW. The output of the correlator banks for all uncompressed range cells constitute the compressed range responses. For the moment we shall not concern ourselves with the small frequency–overlap between the correlator banks for two neighboring uncompressed range cells.

Returning to the problem of range–mismatch, the worst case scenario is for a target that is located at the centre of an uncompressed range cell. In this case, the target–echo samples will be split into two equal halves, each belonging to a different decomposed sub–sequences. Since we have already introduced a bank of correlators to alleviate the problem of frequency–mismatch, the two truncated sub–sequences can each be correlated with the correlator bank associated with the two neighbouring uncompressed range cells and will presumably match one of the frequency bins in the correlator banks. Thus, the net result of having a target situated at the centre of an uncompressed range cell is a loss of integration gain of about 3 dB because only half the number of target samples can be used in the correlation in either correlator bank.

One way to alleviate this problem is to use overlapped sub–sequences where N_s is slightly greater than the value determined from (39) so that samples of a range–displaced target will not be truncated. This means that a slightly longer replicas would have to be used.

There is a limit, however, on how much the subsequences can be overlapped. The purpose of decomposing the composite returns into mutually exclusive sub–sequences is to ensure that target samples with beat frequencies that differ by the amount f_a (see(38)) will not be fed into the same correlator bank, thereby eliminating the ambiguous range response. In fact, the extent of the uncompressed range cell should not be so large that a target at the far end of the uncompressed range cell produces a beat frequency greater than that of a target at the near end by an amount f_a. From (20) and (38), it can be concluded that the length of the transmit pulse segment must not be longer than:

$$\tau_{pmax} = \frac{1}{\mu T_f} \tag{42}$$

if ambiguous range response is to be avoided.

With the above considerations, we can now describe the steps of the modified FMICW processing procedure. It should be emphasized that the procedure described here is intended to provide a general structure of the processor and is not meant to be the finalized version to be used in an operational system. The modified FMICW processing scheme comprises the following steps:

a. For each transmitted pulse segment i, i=0,1,2,...N_p–1, within an FM sweep, divide the received sampled data into a number of M_s subsets of samples, each comprising N_s samples ($\{s_m^i(n)\}$, n=1,2,...,N_s; m=1,2,...,M_s). These N_s samples represent the echo from all the scatterers located inside an uncompressed range cell m. There are M_s uncompressed range cells within the maximum unambiguous range determined by the uncompressed pulse length τ_p and the pulse repetition period T_f:

$$M_s = \frac{T_f}{\tau_p} \tag{43}$$

The number N_s is determined nominally from the sampling frequency f_s and the pulse–segment length τ_p:

$$N_s \approx \tau_p f_s \tag{44}$$

The exact value of N_s depends on how much range–mismatch can be tolerated. If the value determined from (44) is used, there will be a maximum of 3 dB degradation in coherent integration gain for some targets (see discussion earlier in this section).

b. For each of the M_s subsets, correlate the N_s samples with a set of L+1 complex sinusoidal replicas sampled from the functions $r_{m,l}^i(t) = \exp\{j2\pi f_{m,l} t\}$, $l = 0,\pm1,\pm2,...,\pm L/2$.:

$$c_{m,l}^i = \sum_{n=1}^{N_s} s_m^i(n)\, r_{m,l}^i(n) \tag{45}$$

The value of L is determined from (41). For uncompressed range cell m, the frequency of the lth replica is given by:

$$f_{m,l} = \mu m \tau_p + l\Delta F \tag{46}$$

$$l = 0, \pm 1, \pm 2, \ldots, \pm \frac{L}{2}.$$

where ΔF is the resolution of the range transform as defined in (23).

If we assume that the phase of all sinusoidal replicas to be zero at the beginning of the FM sweep period (t=0), at some arbitrary time $t > 0$ the phase would have increased by an amount $2\pi f_r t$, where f_r is the replica frequency. Consequently, the initial phase $\phi_{i,m,l}$ of the sinusoidal replica samples is determined from:

$$\phi_{i,m,l} = 2\pi f_{m,l}(iT_f + m\tau_p) \tag{47}$$

c. Accumulate the correlation results with those of the preceding pulse segments and store in temporary storage:

$$C^i_{m,l} = C^{i-1}_{m,l} + c^i_{m,l} \tag{48}$$

where $C^{i-1}_{m,l} = c^0_{m,l} + c^1_{m,l} + \ldots + c^{i-1}_{m,l}$.

Note: Upper case C represents accumulated quantities, and lower case c represents the correlation obtained for the current pulse segment.

d. Repeat steps a to c for pulse segment No. i+1 until the returns from all N_p pulse segments are processed:

$$C_{m,l} = \sum_{i=0}^{N_p-1} c^i_{m,l} \tag{49}$$

The total correlation results (49) represent the relative strength of the echoes from each of the compressed range cells and can be used for target detection or further signal processing (e.g., Doppler processing) to suppress sea clutter or to further enhance the signal–to–noise–ratio.

2.4.2 Example.

A specific example will serve to clarify the above procedure. Consider an FMICW with the following parameters:

Nominal carrier frequency $f_o = 6.0$ MHz
FM sweep bandwidth B = 375 kHz.
FM sweep period $T_s = 0.5$ sec.
Pulse length $\tau_p = 240$ μsec.
Pulse repetition interval $T_f = 3$ msec
Sampling frequency $f_s = 125$ kHz (Δt=8 μsec per sample)

With the above set of parameters and assuming a maximum target speed of Mach 2, the following values are obtained:

N_p = No. of pulse segments in an FM sweep period = 166.
$\mu = 7.5 \times 10^5$ Hz/sec
$|f_{dmax}| = 26.5$ Hz
$\Delta F = 2$ Hz

The processor structure can be determined as follows:

M_s = No. of uncompressed range cells = 12 (step a)
N_s = No. of samples per range cell = 30 (step a)
L+1 = No. of correlators required
per uncompressed range cell = 117. (step b)

The frequency (in Hz) of the sinusoidal replicas for this example are tabulated in Table 1 for the lth correlator of the mth uncompressed range cell (Step b).

Table 1: Replica frequencies (Hz) of the lth correlator for the mth uncompressed range cell.

m \ l	–58	–57		–2	–1	0	1	2		58
1	64	66	...	176	178	180	182	184	.....	296
2	244	246	...	356	358	360	362	364	....	476
3	424	426	...	536	538	540	542	544	....	566
4	604	606	...	716	718	720	722	724	.....	836
.	.	.	...	.	.	900	.	.	.....	.
.	.	.	...	.	.	.	.	.	.....	.
.	.	.	...	.	.	.	.	.	.....	.
.	.	.	.	.	.	.	.	.	.....	.
12	2044	2046	....	2156	2158	2160	2162	2164	....	2276

The initial phase of the replica segments is dependent on the pulse–segment index i, i=0,1,2,.., N_p–1 (see Figure 9c) and is determined from (47). For example, the initial phase of the 360 Hz correlator (m=2, l=0 in Table 1) for pulse segment #1 is $2\pi(360)(3\times10^{-3}+2\times240\times10^{-6}) = 7.87$ rad.

In a practical system the replica samples will be pre–computed and stored in random access memory to be read by the processor using an address determined from indices i, m and l.

2.4.3 Estimation of computational effort for the modified processing procedure.

It is not very meaningful to compare the computational effort of two processors that do not produce the same output. Nevertheless, we shall do so with the objective of determining whether the modified processing scheme for the FMICW would require excessive amount of extra computational effort over that required for the conventional FFT approach.

We shall consider the specific example of Section 2.3.2. The total number of samples in the time series representing the composite returns in one FM sweep period over the unambiguous range is 60000. This time series can be processed with a 65536–point FFT. The required number of complex multiplications is $16 \times 65536 \approx 1.05 \times 10^6$. A direct calculation of the 65536–point DFT, on the other hand, would require $65536^2 \approx 4.3 \times 10^9$ complex multiplications, a more than three orders of magnitude difference. Now since the sampling rate is 125 kHz, the frequency resolution of the FFT is 125000/65536 = 1.907 Hz; the FFT frequency bins range from 0 to 125 kHz. At the maximum range of 475 km, the maximum beat frequency is $|\mu T_f| = 2250$ Hz. Consequently, 98% of the FFT output is not needed. So the saving in computational effort is about one order of magnitude.

If the modified procedure described in Section 2.3.2 is employed, the number of complex multiplications may be estimated as follows. For each FM sweep period there are N_p pulse segments. The returns from each of these pulses over the unambiguous range are divided into M_s sub–sequences each having N_s complex samples. Each of these sub–sequences are to be correlated with L+1 complex sinusoidal replicas. Hence the total number of complex multiplications is:

$$M = N_p \times M_s \times N_s \times (L+1) \tag{50}$$

Using the parameter values of the above example, we have:

$$M = 166 \times 12 \times 30 \times 117 \approx 7. \times 10^6$$

which is only about seven time greater than that required by the FFT.

Since the direct correlation approach circumvents both the problems of ambiguous range response and that of weak targets being masked by strong targets at close–in ranges, the modified processing scheme is superior to the conventional FFT approach.

3. Performance evaluation of FMICW in HFSWR applications.

In this section, we shall evaluate the performance of the FMICW waveform when it is employed in an HFSWR system. The aim is to provide some qualitative and, if possible, quantitative indication of whether it will yield better performance than a conventional pulsed waveform in HF radar environments. The background interference in HFSWR comprises sea–clutter, noise and other forms of atmospheric disturbance. Interference such as the direct over–head ionospheric reflection and sky–wave interference is beyond the control of the radar. A detailed performance comparison of various waveforms will require a lot more information than is available at this time. We can, however, compare the waveforms on the basis of their detection capability in the presence of sea clutter and noise. The evaluation criteria are given in Section 3.1. Performance in both ship–target and aircraft target–detection applications will be considered.

3.1 Evaluation Criteria.

The relative severity of the effects of sea clutter and external noise on target detection depends on the radar and target characteristics. For example, the relatively low velocity of ship targets produces a Doppler shift in the received echo that falls in the region occupied by sea clutter. As a result the ability of the radar waveform to suppress sea clutter is more important. For aircraft targets whose relatively high velocity produces a Doppler shift that is outside the region dominated by sea clutter, or for all targets at long ranges where noise dominates the background interference, the maximum attainable signal–to–noise ratio of a waveform is important.

Two criteria, namely, the signal–to–noise ratio and the signal–to–sea–clutter ratio will be used to evaluate the FMICW by comparing them with those of a simple unmodulated pulsed waveform.

3.1.1 Signal–to–noise ratio (SNR)

It is essential to specify precisely the context within which we consider SNR. For radar applications, the pertinent value of SNR is the one at the time instant of target detection. For a single pulse, the maximum SNR is attained by passing the received waveform through a filter matched to the transmit waveform and taking a sample of the filter output every τ seconds, where τ is the transmit pulse length for an unmodulated pulse and the compressed pulse length for a modulated pulse. As long as a matched filter is used in the predetection stages of a receiving system, the ability to detect a radar signal is only a function of the energy it contains and is independent of the waveform of the signal as it enters the receiver.

Consider for example a simple unmodulated pulse and a linear FM pulse waveform . For the unmodulated pulse waveform with amplitude A_1 and pulse length T_1, the matched filter for target detection in white Gaussian noise is the well–known integrate–and–dump filter [12], and the SNR is given by:

$$\rho_1 = \frac{A_1^2 T_1}{2N_0} = \frac{E_{b1}}{N_0} \tag{51}$$

where E_{b1} is the energy in the pulse, and N_0 is the one–sided noise density.

Similarly for a linear FM pulse with amplitude A_2 and uncompressed pulse length T_2, the matched filter is a correlator, and the SNR is given by:

$$\rho_2 = \frac{A_2^2 T_2}{2N_0} = \frac{E_{b2}}{N_0} \tag{52}$$

Consequently, the optimum SNR between two waveforms differ on account of the differences in peak power and the pulse length or simply the energy contained in the pulse. We shall compare the waveforms on an equitable basis and require that the two waveforms being compared to have identical average powers. The average power of a radar signal is defined as:

$$P_{av} = \frac{1}{T_f} \int_0^T A^2 \cos^2(2\pi f_o t)\, dt = \frac{A^2 T}{2 T_f} \tag{53}$$

where T is the pulse length and T_f is the pulse repetition interval.

From (51), (52) and (53), we conclude that if two radars transmit two different waveforms with identical average power and PRF, then there is no difference in the attainable SNR between the two waveforms on a single pulse basis. It does not mean, however, that there will not be any difference in SNR between two waveforms when multiple pulses are involved in the detection.

The matched filter concept is not confined to a single pulse. In fact, most of the radar signal processing techniques such as coherent integration and Doppler processing are extensions of the matched filter concept to multiple pulse situations. Take, for example, the case of a bank of Doppler filters that follows the analog–to–digital converter (ADC) of the radar video. In this case we are expecting the sampled data of the echo from a moving target to resemble a sinusoidal waveform. Hence it will match one of the replicas in the Doppler–filter bank. The Doppler filter that matches the echo samples will yield a maximum SNR against white Gaussian noise.

Matched filtering involving multiple pulses is generally referred to as coherent integration. It can be shown [13] that coherent integration over N pulses improves the SNR by a factor of N if the signal component is present in all N pulses and the noise is uncorrelated from one sample to the next. With this broader definition of matched filter, two waveforms can yield different values of SNR even though the single–pulse SNR's are the same. The number of signal samples available for integration could differ between two waveforms because of the difference in the interaction of the waveforms with the target and interference. An example is the so–called range walk problem.

A pulse compression waveform reduces the range cell size so that a high speed target will migrate to a neighboring range cell in a short time, whereas a simple pulsed waveform with the same pulse length would have a much larger range cell, thereby yielding more samples for coherent integration. More will be said about this in Section 3.3.

3.1.2 Signal–to–clutter ratio (SCR).

The received power of an HFSWR from a point target at a given range is determined from the radar equation [14]:

$$P_r = P_t \frac{G_t G_r \lambda^2 F^2 \sigma}{(4\pi)^3 R^4} \tag{54}$$

where P_t = Transmit power in watts
P_r = Received power in watts
G_t = Transmit antenna gain
G_r = Receive antenna gain
λ = Radar wavelength in metres
R = Target range in metres
σ = Target radar cross section in m^2
F^2 = Two–way surface Wave attenuation factor

Sea clutter is a result of scattering from the sea surface which is a distributed target. The SCR is the ratio between the power of the target echo and the total back–scattered power from the sea surface within the radar resolution cell. The area of a radar resolution cell is defined by:

$$A = Rc\frac{\tau}{2}\theta \tag{55}$$

where τ is the pulse length and θ is the azimuthal beamwidth of the radar antenna. Since the sea surface is a distributed target, the range–cell area may be divided into a number of elemental cells each with an area of δA. The elemental cells are assumed to be sufficiently small so that the radar equation for point targets (54) applies.

The RCS for an elemental cell is given by:

$$\delta\sigma = \sigma^{o}\delta A \tag{56}$$

where σ^{o} is the sea–clutter scattering coefficient. The total sea–clutter power from the entire range cell is then obtained from the super–position of the back–scattered power from all the elemental cells.

For the purpose of assessing the impact of the waveforms on sea clutter, we only need an approximated expression for the SCR. We shall assume the following:

(i) the extent of the range cell ($c\tau/2$) is much smaller than the range R.

(ii) within the range cell, the two–way propagation factor F^2 is constant.

Under the above assumptions, the sea–clutter power may be approximated by:

$$P_c = \frac{P_t G_t G_r \lambda^2 F^2 \sigma^{o} \frac{c\tau}{2} \theta}{(4\pi)^3 \ R^3} \tag{57}$$

Hence the SCR is approximately given by:

$$SCR = \frac{\sigma}{\sigma^{o} R \frac{c\tau}{2} \ \theta} = \frac{\sigma}{\sigma^{o} A} \tag{58}$$

For an unmodulated pulse, τ is simply the transmitted pulse length. For an FM waveform, τ is the compressed pulse length.

It can be seen that the signal power does not appear explicitly in the expression of the SCR. Consequently, the SCR cannot be increased by increasing the transmit power. It can only be increased through a reduction in the range–cell size.

3.2 FMICW in ship detection application.

The primary consideration for a waveform in ship detection is its capability to suppress sea clutter. As discussed in Section 3.1.3, the effective SCR can be increased only through a reduction of the range cell size. Intuitively, therefore, a pulse compression type of waveform would have an advantage over a simple pulse waveform for target detection in a sea–clutter dominated environment. Let us consider a specific case. Assume the following sets of parameter values for the pulsed system and the FMICW systems.

Parameters	simple pulsed waveform	FMICW
Peak Power	50 kW	10 kW
Frequency	6.0 MHz	6.0 MHz
PRF	333.33 Hz	333.333 Hz
Pulse length	50 μsec	250 μsec
FM Sweep Bandwidth	–	375 kHz
FM Sweep period	–	0.5 sec.
Integration period	128 sec.	128 sec.

The two waveforms have identical average power. For each integration period, there are 42666 pulses. For the unmodulated pulse, the processing is performed with a DFT on the 42666–point time series. This yields a Doppler resolution of $\Delta f = 333.33/42666 = 0.00781$ Hz. The extent of the range cell for this waveform is simply $c\tau/2 = 7.5$ km.

For the FMICW waveform, the 42666 pulses are divided into 256 FM sweeps each comprising 166 pulse segments. The 166 pulse segments in each FM sweep are pulse–compressed to yield the range response of compressed range cells having an extent of approximately 400 m. After pulse compression the effective Doppler domain is reduced to about 2 Hz (see Section 3.3). For each compressed range cell, the responses from successive FM sweeps form a time series. Since there are 256 FM sweeps, the resulting time series has 256 samples. Hence the Doppler resolution is $2/256 = 0.00781$ Hz which is identical to the value for the simple pulse waveform.

Since the SCR varies inversely with the range–cell size, the improvement in SCR for the FMICW over that of the simple pulsed waveform is 7500/400 = 18.75 or 12.73 dB. This improvement, however, is for a stationary target. For moving targets the realizable improvement on the SCR will decrease because of the decrease in signal power due to the target's range migration. For example, a ship travelling towards the radar at 20 knot will remain inside a 400 m range cell for about 39 second. This means that a coherent integration time longer than 39 seconds may not produce the optimum SCR. Nevertheless, the FMICW still have a significant advantage over the simple pulsed waveform under sea–clutter dominated conditions due to its lower peak power requirement, a higher up–date rate and a higher range resolution.

3.3 FMICW in aircraft detection application.

There is an implicit trade–off in the pulse compression operation for an FMICW waveform. This trade–off is in terms of reducing the Doppler domain in exchange for an increased range resolution. This may be visualized by examining Figure 10. In Figure 10a, transmitted pulse segments of a number of FM sweep periods are shown. The composite returns (not shown) from each pulse segment are pulse–compressed as described in Section 2.3.2 to yield the range response. After the pulse compression operation, the result is a number of correlator outputs representing the magnitude of the return from various compressed range cells up to the maximum unambiguous range.

For a given compressed range cell, the magnitude yielded from successive FM sweeps will form a time series. This time series can be Doppler–analyzed to enhance the SNR for targets having various Doppler shifts. Since it takes the entire FM sweep period to produce one sample of these time series (see Figure 10b), the effective sampling frequency and consequently, the Doppler domain, is $1/T_s$. If the FM sweep period T_s is long, the resulting Doppler domain can becomes very narrow as shown in Figure 10c. For example, if $T_s = 0.5$ second, then the Doppler domain of the time series is 2 Hz.

By contrast, the Doppler domain of a time series of echoes from an unmodulated pulse train is simply the radar's PRF (see Figure 10d and 10e). It can be seen that the sea clutter spectrum occupies a tiny fraction of the entire Doppler domain. For aircraft targets, the Doppler shift is relatively high due to their high velocities. A reduction in the Doppler domain will result in the aliasing of the the target signal onto the Doppler region

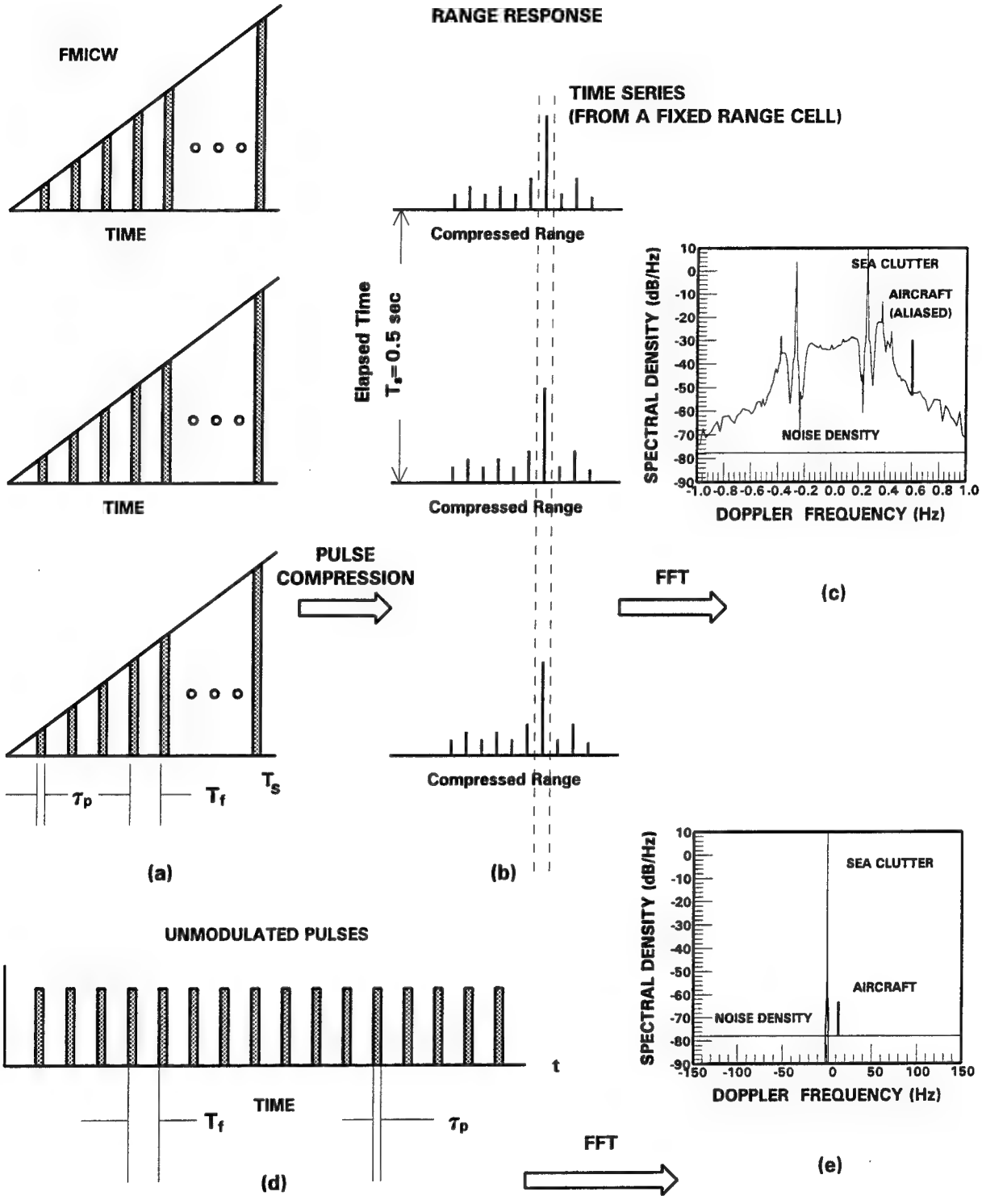

Figure 10. Comparison of detection of high-speed targets between a specific FMICW and an unmodulated pulse waveform: (a) FMICW pulse train, (b) FMICW range response, (c) FMICW Doppler output, (d) Unmodulated pulse train, and (e) Doppler output of unmodulated pulse train.

occupied by the sea clutter. This has two detrimental effects. The first is that, instead of competing with external noise for detection, the target signal is competing against sea clutter for detection which, in most cases, is substantially higher in magnitude than external noise.

The second is the related problem of maintaining a low probability of false alarm while achieving the desired probability of detection. To set the appropriate detection threshold, one needs to know the probability density of the background interference. If the background interference is external noise, then for Doppler frequencies outside the region occupied by the sea clutter, the Rayleigh or exponential (depending on whether processed output is proportional to voltage or power) distributions may be assumed. It is generally accepted that external noise has a white spectrum which implies that the noise distribution is Doppler–independent. Consequently, the process of determining the appropriate detection threshold setting is greatly simplified.

If, on the other hand, the background interference is sea clutter, the detection threshold would be a function of the sea–clutter probability density which is Doppler–dependent. For targets whose Doppler shift is in the vicinity of the Bragg lines [15], the threshold setting will necessarily be high, thereby reducing the detection probability. Otherwise the false alarm regulation performance of the radar will be compromised.

Another potential problem arising from the reduced range cell size is the so–called range walk problem. The substantially higher velocity of aircraft relative to those of ships means that it takes a much shorter time for an aircraft to traverse a range cell. If the size of the range cell is further reduced through pulse compression, the coherent integration time will be decreased proportionately. This is because coherent integration is performed on samples representing the same range cell taken at contiguous time instants. There will be no coherent integration gain if the signal is not present.

Consider the FMICW waveform as discussed in Section 2.3.2. The compressed range cell size is about 400 m. A Mach 1 (331m/sec) target will only remain in the 400 m range cell for slightly more than one second. On the other hand, the extent of the range cell for an unmodulated pulse is $cT_p/2$, where T_p is the pulse length. With a 50 μsec pulse, the extent of the range cell is 7.5 km. Thus the same target will still be within the 7.5 km range cell in 22 seconds.

For the FMICW waveform described in Section 2.3.2, coherent integration of the range samples from the same range cell may not provide optimum results for aircraft targets. Some form of target–trajectory model which postulates the position and velocity of the target would be required to permit integration of the samples from different range cells over an extended period of time. Since there is a range–Doppler ambiguity in the pulse–compressed result over one FM sweep period, there will be an uncertainty regarding the target velocity estimated from the subsequent Doppler–processed results. This will further complicate the detection process.

4. Summary and conclusions.

In this section we shall attempt to arrive at some conclusions regarding the merits of the FMICW waveform in ship and aircraft detection. As in many real life situations, there are no clear–cut answers. It is hoped that by presenting various advantages and disadvantages and cost estimation, informed decision on the merits of the waveform can be made.

4.1 Effect of the waveform on SNR.

The SNR of a radar system, as the name implies, is a function of signal power and the amount of noise power that is permitted to get into the receiver pass–band. In the pre–detection stages, the SNR is a function of the received signal power and the receiver bandwidth, assuming white Gaussian noise. The available signal power to a radar receiver is often ill–defined because the received power is a function of range, radar cross section and other factors dependent on the characteristics of the channel. Fortunately, for radar applications, the pertinent SNR is the value at the detection stage which is usually the output of the matched filter.

It has been shown that, if two waveforms with identical average power are processed by the appropriate matched filter then there is no difference in the attainable SNR on a single pulse basis. The overall effect of the FMICW waveform on SNR in multiple pulses situation is dependent on the target characteristics. The attainable SNR could decrease for high–speed targets due to range walk arising from a reduced range cell size.

4.2 Effect of the waveform on sea clutter.

As discussed in Section 3.2 the primary consideration for a waveform for ship detection is its capability to suppress sea clutter. Unlike the SNR, the SCR cannot be increased by increasing the transmit power. It can only be increased through a reduction in the range cell size. Pulse compression waveform is superior to a simple pulsed waveform in this respect. The reason is that pulse compression increases the range resolution, thereby reducing the sea–clutter power through a reduction of the range cell size.

4.3 Hardware considerations for FMICW implementation.

4.3.1 Transmitter and receiver

A modulated pulse of longer length has an advantage over an unmodulated pulse of shorter length in terms of the peak power requirement for the radar. In order to attain the same SNR, an unmodulated pulse with shorter pulse length must compensate for the reduced average power by increasing the peak power. Because of the lower peak power requirement for the FMICW waveform, it is reasonable to assume that there would be a cost as well as a reliability advantage in the transmitter over that employed for the simple pulsed waveform.

There is also an advantage in the receiver employing FMICW in terms of the instantaneous bandwidth requirement. Consider a simple pulsed waveform of 50 μsec and an FMICW of 250 μsec. The average powers for the two waveforms are assumed to be identical. The theoretical instantaneous bandwidths for the 50 μsec and the 250 μsec pulses are 20 kHz and 4 kHz respectively. The FMICW receiver will require additional bandwidth to accommodate the frequency shift produced by a target at the maximum unambiguous range.

Consider an FM sweep rate of 750 kHz/sec and a maximum unambiguous range of 450 km. The frequency shift due to a target at 450 km is calculated from (34) to be 2250 Hz. Therefore, a conservative design of 8 kHz would suffice. This is still lower than the 20 kHz required for the 50 μsec pulse.

4.3.2 Effect of the waveforms on signal processing.

From the considerations presented in Section 2.3.3, there is some increase in computational effort in the processing of FMICW over that required for processing an unmodulated pulse waveform. However, this increase in computational effort also yields an increase in the radar's range resolution. Compared to the conventional FFT approach of processing the FMICW, the increase in computational effort is less than one order of magnitude. No significant increase in the complexity of the processor is anticipated since the processor structure for the modified FMICW processing scheme is essentially that of a complex correlator.

4.4 Conclusion

As discussed in Section 3.3, there is an implicit trade–off in the pulse–compression operation of the FMICW waveform. The excess Doppler domain in which no targets are expected to be found is traded off in exchange for an increased range resolution. For ship detection application, it is obvious that the FMICW is superior to the simple pulsed waveform because it (i) enhances the signal–to–clutter ratio, (ii) provides a finer range resolution and (iii) requires a lower peak power. These advantages are there because the Doppler shift of ship targets is low compared with the radar's PRF. For example, at a carrier frequency of 6 MHz, the Doppler shift of a ship travelling at a speed of 40 knots is only 0.82 Hz. Assuming a PRF of 300 Hz, the maximum Doppler shift for ship targets only occupies about 0.5% of the total Doppler domain of 300 Hz. Consequently, 99.5% of the excess Doppler domain can be traded in exchange for an increased range resolution.

For aircraft detection application, however, the advantage of the FMICW is less obvious. The reasons are as follows. First, the Doppler shifts of aircraft targets are much greater than those of ship targets. For example, a Mach 2 target will produce a Doppler shift of about 26.5 Hz at a radar frequency of 6 MHz. To accommodate both approaching and receding targets, a total Doppler domain of 53 Hz is required. Again assuming a 300 Hz PRF, this Doppler domain amounts to about 18% of the PRF. Consequently, there is a lot less excess Doppler domain to be traded off for increased range resolution. Second, by increasing the range resolution, the probability of target range walk is increased. Consequently, the detection performance for high speed targets will be degraded.

Theoretically, higher pulse–compression–ratio may be obtained by increasing the FM sweep rate within a FM sweep period. However, this requires a higher instantaneous bandwidth for both the transmitter and receiver.

Again consider the example of Section 3.2. For the unmodulated 50 μsec pulse, the range extent of the resolution cell is 7.5 km and the minimum instantaneous bandwidth is 20 kHz. For an FMICW waveform to yield an unambiguous Doppler domain of 53 Hz, the FM sweep period cannot be longer than $1/53 = 18.87$ msec. To obtain a compressed range cell of 400 m, the 375 kHz bandwidth must be swept in 18.87 msec. Hence the FM sweep rate is $\mu = 375 \times 10^3/18.87 \times 10^{-3} \approx 20$ MHz/sec. For a pulse–segment length of $\tau_p = 240$ μsec, the change in the carrier frequency is $|\mu\tau_p|$ =4.8 kHz. However, the maximum beat frequency of the echo from a target at the maximum unambiguous range of 450 km is $|\mu T_f| \approx 60$ kHz. To accommodate all possible targets within the unambiguous range, the required instantaneous bandwidth of the receiver will be well over 60 kHz. With a wider instantaneous bandwidth, the SNR will be degraded.

Another problem associated with a shorter FM sweep period is the reduction in the number of pulses available for pulse compression. For a 0.5 sec FM sweep period and a 3 msec PRI, there are 166 pulses which can be used in the pulse compression operation. For the 18.87 msec FM sweep period and 3 msec PRI, there are only 6 pulses. Consequently, the coherent integration gain of the pulse–compressed results is reduced significantly

Overall, it may be concluded that the FMICW is superior to an unmodulated pulse waveform for ship–detection application. For aircraft detection, the advantage of the FMICW is perhaps marginal. It depends on the parameters chosen for the system. Generally the FM sweep rate and the sweep period must be chosen so that the resulting Doppler bandwidth would be unambiguous for the anticipated aircraft speed.

An important element has been left out in the above consideration. That is the susceptibility of the waveforms to co–channel interference. Intuitively, one would expect that a simple pulsed waveform would be more susceptible to co–channel interference than an FM signal because the interference affects the FM signal only when the carrier frequency coincides with the band the interference is in, which is only a fraction of the pulse train; whereas, the interference will affect the entire unmodulated pulse train.

On the other hand, if the receiver possesses some degrees of frequency agility, then it is not obvious which of the two waveforms will be more resistant to co–channel interference. Since a simple pulsed waveform occupies a relatively narrow bandwidth, it should be relatively easy for the transmitter to locate a channel that is free of interference. The FMICW waveform, on the other hand, requires a contiguous bandwidth that is in the order of several hundred kHz. Hence, the probability of encountering interference in some channel inside that band is higher. Here frequency agility does not help because one would have to locate a contiguous band of frequencies that is free of interference.

A comprehensive evaluation of the interference aspect of the two waveforms is beyond the scope of this report. It will required a detail simulation with precise information on the probability distribution of interference in the frequency band under consideration.

5. References

[1] E.C. Jordan, "Electromagnetic waves and radiating systems," Prentice–Hall, Inc., Englewood Cliffs, N.J., 1962, p. 618.

[2] A.W. Rihaczek, "Principles of high–resolution radar," Mark Resources, Inc, 1977.

[3] C.E. Cook and M. Bernfeld, "Radar signals – An introduction to theory and application," Academic Press, New York, New York, 1967.

[4] R.S. Berkowitz, Ed.,"Modern Radar – analysis, evaluation and system design," John Wiley & Sons, Inc., New York, 1965.

[5] A.G. Stove, "Linear FMCW radar techniques," IEE Proceedings–F, Vol. 139, No.5, October 1992, pp. 343–351.

[6] S.O. Piper (J.A. Scheer and J.L. Kurtz, Ed.), "Coherent Radar Performance Estimation, Chapter 12: Frequency–modulated continuous wave systems," Artech House, Boston, 1992, pp. 289–313.

[7] D.G.C. Luck, "Frequency modulated radars," McGraw–Hill Book Company, New York, 1949.

[8] R.J. Schwarz and B. Friedland,"Linear Systems," McGraw–Hill Book Company, New York, New York, 1965.

[9] J.W. Cooley and J.W. Tukey, "An Algorithm for machine calculation of complex Fourier series," Math. Computation, vol. 19, April 1965, pp.297–301.

[10] L.R. Rabiner and B. Gold, "Theory and application of digital signal processing," Prentice–Hall, Inc., Englewood Cliffs, N.J., 1975, pp. 194–204.

[11] R.H. Khan and D.K. Mitchell, "Waveform analysis for high–frequency FMICW radar," IEE Proceedings–F, Vol. 138, No. 5, October 1991, pp. 411–419.

[12] J.M. Wozencraft and I.M. Jacobs, "Principles of communication engineering," John Wiley & Sons, Inc., New York, 1965.

[13] M.I. Skolnik, Ed., "Radar handbook," McGraw–Hill Book Company, New York, New York, 1970.

[14] J.M. Headrick (M.I. Skolik, Ed.), "Radar Handbook, 2nd Edition – Chapter 24: HF over–the horizon radar," McGraw–Hill Book Company, New York, New York, 1990, p. 24.3.

[15] D.E. Barrick, J.M.Headrick, R.W.Bogle and D.D. Crombie, "Sea Backscatter at HF: interpretation and utilization of the echo," Proc. IEEE, vol. 62, June 1974, pp. 673–680.

6. Acknowledgement

The author thanks Dr. R.H. Khan of C–CORE for his communication on the formulation of his FMICW processing procedure and Dr. T.N.R. Coyne for useful discussions and reviewing of the manuscript.

DOCUMENT CONTROL DATA

(Security classification of title, body of abstract and indexing annotation must be entered when the overall document is classified)

1. ORIGINATOR (the name and address of the organization preparing the document. Organizations for whom the document was prepared, e.g. Establishment sponsoring a contractor's report, or tasking agency, are entered in section 8.)

Defence Research Establishment Ottawa
3701 Carling Ave., Ottawa, Ontario, K1A 0Z4, Canada

2. SECURITY CLASSIFICATION (overall security classification of the document including special warning terms if applicable)

UNCLASSIFIED

3. TITLE (the complete document title as indicated on the title page. Its classification should be indicated by the appropriate abbreviation (S,C or U) in parentheses after the title.)

Evaluation of the FMICW waveform in HF surface radar applications (U)

4. AUTHORS (Last name, first name, middle initial)

Chan, Hing C.

5. DATE OF PUBLICATION (month and year of publication of document)	6a. NO. OF PAGES (total containing information. Include Annexes, Appendices, etc.)	6b. NO. OF REFS (total cited in document)
January 1994	53	15

7. DESCRIPTIVE NOTES (the category of the document, e.g. technical report, technical note or memorandum. If appropriate, enter the type of report, e.g. interim, progress, summary, annual or final. Give the inclusive dates when a specific reporting period is covered.)

DREO Report

8. SPONSORING ACTIVITY (the name of the department project office or laboratory sponsoring the research and development. Include the address.)

Defence Research Establishment Ottawa, 3701 Carling Ave., Ottawa, Ontario K1A 0Z4

9a. PROJECT OR GRANT NO. (if appropriate, the applicable research and development project or grant number under which the document was written. Please specify whether project or grant)	9b. CONTRACT NO. (if appropriate, the applicable number under which the document was written)
041LR	

10a. ORIGINATOR'S DOCUMENT NUMBER (the official document number by which the document is identified by the originating activity. This number must be unique to this document.)	10b. OTHER DOCUMENT NOS. (Any other numbers which may be assigned this document either by the originator or by the sponsor)
DREO Report No. 1219	

11. DOCUMENT AVAILABILITY (any limitations on further dissemination of the document, other than those imposed by security classification)

- (X) Unlimited distribution
- ( ) Distribution limited to defence departments and defence contractors; further distribution only as approved
- ( ) Distribution limited to defence departments and Canadian defence contractors; further distribution only as approved
- ( ) Distribution limited to government departments and agencies; further distribution only as approved
- ( ) Distribution limited to defence departments; further distribution only as approved
- ( ) Other (please specify):

12. DOCUMENT ANNOUNCEMENT (any limitation to the bibliographic announcement of this document. This will normally correspond to the Document Availabilty (11). However, where further distribution (beyond the audience specified in 11) is possible, a wider announcement audience may be selected.)

UNLIMITED

UNCLASSIFIED

SECURITY CLASSIFICATION OF FORM

13. ABSTRACT (a brief and factual summary of the document. It may also appear elsewhere in the body of the document itself. It is highly desirable that the abstract of classified documents be unclassified. Each paragraph of the abstract shall begin with an indication of the security classification of the information in the paragraph (unless the document itself is unclassified) represented as (S), (C), or (U). It is not necessary to include here abstracts in both offical languages unless the text is bilingual).

(U) The operation and performance of the Frequency Modulated Interrupted Continuous Wave (FMICW) waeform in ship and aircraft detection using high frequency surface wave radar are analyzed. A modified processing scheme for the FMICW waveform which circumvents the problem of ambiguous range response is presented. The increase in hardware complexity for the modified processing scheme is moderate. Two measures: (a) the signal-to-noise ratio and (b) the signal-to-clutter ratio are used to evaluate the performance of the FMICW. It is concluded that the FMICW is supreior to the simple pulsed waveform in ship-detection application. For aircraft detection, the advantage of the FMICW is marginal. Parameters optimized for ship-detection application will not be optimal for aircraft-detection application because of their much higher velocity which exacerbates the range-walk problem.

14. KEYWORDS, DESCRIPTORS or IDENTIFIERS (technically meaningful terms or short phrases that characterize a document and could be helpful in cataloguing the document. They should be selected so that no security classification is required. Identifiers, such as equipment model designation, trade name, military project code name, geographic location may also be included. If possible keywords should be selected from a published thesaurus. e.g. Thesaurus of Engineering and Scientific Terms (TEST) and that thesaurus-identified. If it is not possible to select indexing terms which are Unclassified, the classification of each should be indicated as with the title.)

HIGH FREQUENCY RADARS, SURFACE WAVE, HF RADARS, PULSE COMPRESSION, FREQUENCY MODULATION, CONTINUOUS WAVE, FM RADARS, CW RADARS